Storage Management in a Shared Solar Environment with Time-Varying Electricity Prices

Johann Leithon, *Member, IEEE,* Stefan Werner, *Senior Member, IEEE,* and Visa Koivunen, *Fellow, IEEE*

***Abstract*—Internet of Things (IoT) technologies will enable smart energy planning, which in turn will expedite the adoption of renewable energy (RE). In this paper, we propose a mathematical framework to optimize the use of RE in a shared solar environment featuring households with access to several RE generators. We consider location and time-dependent electricity prices, and formulate an optimization problem to minimize the energy cost incurred by the households over a finite planning horizon. The proposed framework accounts for transmission losses and battery inefficiencies. We then proposed two approaches to solve the formulated optimization problem. The first approach is based on quadratic programming, and is used to obtain a precision-controllable solution, requiring discretization in time and convex relaxation. The second approach is based on variational methods, which are used to tackle the problem directly in continuous time, thus obtaining a solution in closed form after introducing reasonable simplifications. To ensure full cooperation, we finally derive a fair energy allocation policy, which allocates RE to each household in proportion to its capital investment. The obtained analytical results allow us to evaluate the relationship between achievable performance, RE production, transmission losses and price variability. Extensive simulations are used to verify the derived analytical results, illustrate the characteristics of the proposed strategies and compare their achievable performance.**

***Index Terms*—Storage management, shared solar, quadratic programming, variational methods, heating loss.**

I. Introduction

INTERNET OF THINGS (IoT) technologies will enhance the current data collection infrastructure, which will allow us to optimize resources and eliminate inefficiencies. For example, IoT-enabled decision making can be used for smart energy planning. Within buildings, IoT technologies can be used for energy monitoring and automation [1]. At a city-scale, IoT technologies can help to reduce pollution and traffic congestion [2], modernize the power grid [3], and expedite the adoption of renewable energy (RE) [4], [5].

By increasing the use of RE, cities can reduce their dependency on contaminating power sources such as fossil fuels. However, not every household is able to afford the deployment of wind turbines or solar panels in their rooftops. As a result, sharing RE generation facilities has gained popularity in recent years [6]. Through models such as Shared Solar [7], households unable to afford their own RE generators can team up with their neighbors to share RE infrastructure, thus establishing localized distribution systems, often referred to as microgrids [8]. In this context, optimization strategies can be devised to ensure that participants meet their energy requirements at the lowest economical and environmental costs [9]–[11].

In this paper we develop a mathematical framework to devise RE management strategies for cooperating households with shared access to RE generation sites. We specifically consider a geographical region with $M > 0$ households and $N > 0$ RE generation sites, where each household is potentially connected to all the RE generation sites. The proposed framework accounts for distance- and resistance-dependent power losses in the transmission lines, and battery charging and discharging inefficiencies at each RE generation site. By assuming location- and time-dependent electricity prices, we formulate an optimization problem to minimize the energy cost incurred by all the participating households over a finite planning horizon.

Given the nature of the constraints involved, the formulated problem is non-convex. We thus propose a convex relaxation and two approaches to solve the simplified optimization problem. The first approach is based on quadratic programming (QP) techniques and discretization in time. We then refer to this approach as the QP-based RE optimization (QP-REO) strategy. The second approach is based on the theory of calculus of variations (CoV). We refer to this approach as the CoV-based RE optimization (CoV-REO) strategy.

A. Related Works

There are several works on RE management in the literature. However, very few of them account for power losses in connecting lines, multiple households and RE generation sites, time- and location-dependent electricity prices, and battery charging/discharging inefficiencies. In this section we comment on some of the most prominent works on the topic.

Energy management strategies targeted at associations of users have been proposed in [9], [12]–[25]. Some of these works assume full cooperation from participating users, e.g., [12], [14], while others use game theory to account for participants with conflicting objectives [9], [16], [20]. In some of these works, the RE generation and storage operations take place at the users' site [9], [12], [14], [16], [20], while others assume centralized RE generation [21], or centralized energy storage [15], [17]. Most of these works ignore power transmission losses [9], [12], [13], [15]–[17], [20], while few of them use the well established quadratic [22], [24], or

J. Leithon and V. Koivunen are with the Department of Signal Processing and Acoustics, Aalto University, e-mail: {johann.leithon, visa.koivunen}@aalto.fi. S. Werner is with the Department of Electronic Systems, Norwegian University of Science and Technology, e-mail: stefan.werner@ntnu.no. This work was supported in part by the Academy of Finland under Grant 296849.

linear [23] models to estimate heating loss. Some of these works assume a microgrid environment, where loads and RE generation are aggregated [13], [24].

The works listed above propose energy management strategies from the end-user perspective. Works such as [26] and [27] investigate the energy management problem from the perspective of the utility company, i.e., targeting to minimize generation costs. In [28] and [29] social welfare maximization strategies are proposed. These strategies account for both, utility's and consumer's goals. Among these, only [27] and [28] account for transmission losses in their models. Other RE management strategies available in the literature include [30]–[34], where greedy RE management strategies are proposed at an individual level.

To the best of our knowledge, there are not works in the literature proposing energy management strategies for households with shared RE generators, which are aware of time-varying electricity prices, and power loss dissipation through connecting lines and in energy storage devices (ESDs). Many of the works on multi-user energy management use game theory to determine the actions of the participants and the corresponding equilibrium point. Our perspective in this paper is different because we first optimize the RE consumption rate of each household. Then we propose a fair energy allocation policy to ensure full household cooperation. Finally, we discuss the ownership distribution that optimizes performance.

B. Contributions and Organization

The contributions of this work are the following: First, we propose a mathematical framework to optimize the use of RE across households featuring location- and time-varying electricity prices and loads. The proposed framework takes into account the power loss incurred when the energy is transported from the generation site to the loads. These power losses are distance- and resistance-dependent. The model is general, as it accounts for an arbitrary number of households and generation sites.

Second, we propose two approaches to solve the formulated optimization problem: The first approach is based on quadratic programming techniques and can be used to obtain a precision-controllable solution in the discrete-time domain. The second approach is based on variational methods and results from applying the Euler-Lagrange optimality condition to the original problem formulation in continuous time. This method provides a solution in closed form, which allows us to get a deeper insight into the optimal RE consumption strategy. Specifically, by using the results obtained through variational methods in continuous time, we determine the optimal RE generation capacity in each site. The result is provided in closed form, and illustrates the trade-off between maximizing the use of RE and minimizing the power loss incurred in the transmission.

Third, we propose a fair energy allocation strategy which seeks to ensure full cooperation among the participating households. The proposed energy allocation strategy is described as fair because it seeks to allocate RE in proportion to each household's initial investment in the shared infrastructure. Enforcing this energy allocation policy incurs a performance degradation,[1] which we then minimize by establishing the optimal ownership distribution across participating households. The proposed ownership allocation is based on the concept of dynamic asset allocation [35], which seeks to adjust ownership share across households in response to predicted RE generation and load.

The results presented in this paper can be used for energy planning purposes. For example, the results obtained reveal an RE generation threshold,[2] above which no further cost reduction can be achieved due to transmission loss. Moreover, the expressions derived with the CoV-REO strategy can be used to reduce the computational complexity of forecasting-based online RE management algorithms [36].

This paper is organized as follows: Sec. II presents the system setup describing each of its elements and the assumptions behind the models used. We formulate the main optimization problem in Sec. III. In Sec. IV we describe the proposed solutions. In Sec. V we present our proposed energy allocation strategy and the ownership distribution that minimizes performance degradation. In Sec. VI we analyze numerical results and in Sec. VII we discuss the conclusions of this study.

C. Notation

Vectors are presented with lower case bold letters. The ith element of vector $\boldsymbol{a}$ is denoted by $a(i)$. Matrices are denoted by using upper case bold letters. The row vector of M ones is denoted by $\mathbf{1}_M$. The transpose of matrix $\mathbf{A}$ is written as $\mathbf{A}^\intercal$.

$L_m(\cdot)$, $\boldsymbol{\ell}_m$	Power consumed by the mth household
$P_m(\cdot)$, $\boldsymbol{p}_m$	Energy prices offered to the mth household
$D_{m,n}(\cdot)$, $\boldsymbol{d}_{m,n}$	Renewable power drawn by the mth household from the nth generator
$J_n(\cdot)$, $\boldsymbol{\jmath}_n$	Renewable energy (RE) available at the nth RE generation site
$\preceq$	Element-wise $\leq$
$\otimes$	Kronecker product
$\mathsf{dg}(\mathbf{v})$	Diagonal matrix with $\mathbf{v}$ in its diagonal

II. System Model

A. Power Connectivity, Planning Horizon, and Design Variables

We consider a set of M grid-connected households deployed across a finite geographical area. The planning horizon is $[0, S]$ where $S > 0$ is an arbitrary positive real number. The power consumed by the mth household at time $\tau \in [0, S]$ is denoted by $L_m(\tau) : [0, S] \to [0, L_{\max}]$, where $L_{\max}$ denotes the maximum power that the household can consume.

We consider a set of N RE generators, which are deployed across different locations to ensure statistical diversity [37]. Each generation site is equipped with a single ESD.

[1] Adding constraints to an existing optimization problem restricts its feasible space. Therefore, the performance obtained within the more restricted feasible set is lower than that obtained in the less restricted space.

[2] This threshold is established in terms of the duration of the planning period, the resistance and length of the connecting lines, and the operational voltage.

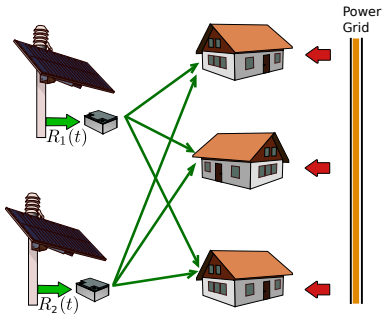

Fig. 1. Cooperative RE sharing system with $N = 2$ generation sites and $M = 3$ households.

The power drawn by the mth household from the nth RE generator is denoted by $D_{m,n}(\tau) : [0, S] \to [0, L_m(\tau)]$. Each household may potentially have access to all the available RE generators. Power connectivity between a household m and an RE generation site n is established when the resistance per unit length of the connecting power line, and denoted by $\rho_{m,n}$, is finite, i.e., $\rho_{m,n} < \infty$. The RE generation sites are not directly connected to each other. For illustration purposes, a network of $M = 3$ households and $N = 2$ RE generation sites is shown in Fig. 1.

B. Objective Function and Transmission Losses

The power transmission losses are caused by the resistance of the connecting lines. Let $\rho_{m,n}$ denote the resistance of the lines per unit length, hence the resistance of the line connecting the mth household and the nth RE generator is $\rho_{m,n}\mathsf{dis}_{m,n}$, where $\mathsf{dis}_{m,n}$ is the corresponding distance between the two points. The current flowing through the line is $\frac{D_{m,n}(\tau)}{\mathsf{V}}$, where V is the operating voltage. Hence, the total power loss PL, incurred over the time interval $[0, S]$ can be written in terms of the $D_{m,n}(\tau)$'s as follows:

$$\mathsf{PL} = \sum_{n=1}^{N}\sum_{m=1}^{M} \rho_{m,n} \int_0^S \mathsf{dis}_{m,n} \left(\frac{D_{m,n}(\tau)}{\mathsf{V}}\right)^2 d\tau. \quad (1)$$

The objective of our proposed strategies is to minimize the cost incurred by all the participating households over the specified planning horizon. To achieve this, we define the objective of our optimization problem as follows:

$$\chi = \sum_{m=1}^{M} \int_0^S P_m(\tau) \left\{ L_m(\tau) - \sum_{n=1}^{N} \left[D_{m,n}(\tau) - \rho_{m,n}\mathsf{dis}_{m,n} \left(\frac{D_{m,n}(\tau)}{\mathsf{V}}\right)^2 \right] \right\} d\tau, \quad (2)$$

where $P_m(\tau)$ denotes the prices offered to the mth households. The pricing functions $P_m(t)$ take on non-negative values for all $t \in [0, \infty)$, and for all $m \in \mathbb{N}$. The pricing functions can be defined in advance by the utility company following the policies that they deem appropriate. For example, in a demand response scenario, these prices can be chosen to encourage certain energy consumption habits, e.g., reducing power consumption during peak hours, etc. Price variations across location are considered to ensure generality. Our objective will thus be to minimize the cost function χ by carefully designing the $D_{m,n}(\tau)$'s.

C. Energy Storage Devices

All the ESDs in the system are characterized by:

1) Charging/discharging losses: The charging/discharging losses are proportional to the power charged to or discharged from the ESD. The charging/discharging efficiency rates of the nth ESD are respectively α_n and β_n, which satisfy $0 < \alpha_n \leq 1$ and $0 < \beta_n \leq 1$. A lossless charging (discharging) operation happens when $\alpha_n = 1$ ($\beta_n = 1$).

2) ESD dynamics: The energy available at the nth ESD is denoted by $J_n(\tau)$, and evolves according to:

$$J_n(\tau) = J_n(0) + \int_0^\tau \left[\alpha_n R_n(x) - \frac{1}{\beta_n} \sum_{m=1}^{M} D_{m,n}(x) \right] dx, \quad (3)$$

where $J_n(0) \geq 0$ is the energy initially available in the battery, and $R_n(\tau)$ is the renewable power charged to the ESD, which is within the charging rate allowed.[3] The term $\frac{1}{\beta_n}\sum_{m=1}^{M} D_{m,n}(x)$ denotes the total power discharged from the nth ESD. As seen in (3), the ESD acts as an energy accumulator, as it integrates the net power flowing through its terminals.

3) Limited storage capacity: The capacity of the nth ESD is denoted by $\Psi_n \in \mathbb{R}_+$. Therefore, the $D_{m,n}(\tau)$'s must be such that $0 \leq J_n(\tau) \leq \Psi_n, \forall\ \tau,\ \forall\ n$.

4) Limited charging/discharging rates: Each ESD has a limited charging/discharging rate, expressed as the maximum amount of energy that can be injected-to/drawn-from the ESD in each time instant. The maximum discharging rate that the nth ESD can handle is $q_{D,n}$ power units. Therefore,

$$\sum_{m=1}^{M} D_{m,n}(\tau) \leq q_{D,n},\ \forall\ \tau,\ \forall\ n. \quad (4)$$

The renewable power charged to the ESD, and denoted by $R_n(t)$ is within the charging rate allowed. This means that RE generation above the maximum charging rate is discarded.

5) Continuous energy level: To account for future planning periods, we can optionally let:

$$J_n(0) = J_n(S),\ \forall\ n, \quad (5)$$

which ensures continuity of the energy level across optimization periods. Constraints (5) restrict the consumption of RE so that it matches the amount of energy generated over the optimization period $[0, S]$. This type of constraint has been enforced in [38].

D. Information Requirements, Decision Making and Household Participation

The strategies proposed in this paper rely on information exchange infrastructure. In particular, participating households

[3]That is, $R_n(\tau) = \min\{q_{C,n}, \tilde{R}_n(\tau)\},\ \forall\ \tau$, where $q_{C,n}$ is the largest charging rate allowed at the nth RE generation site, and $\tilde{R}_n(\tau)$ is the produced power at the nth RE generation site.

and RE generation sites need to share information concerning power consumption and RE production. This information exchange is realized through a communication architecture composed of a control center (CC) and several smart meters deployed across households and RE generation sites. The function of each of these components is explained in [39], [40]. Moreover, the smart meters have communication and controlling capabilities over power switching devices [41]. That is, the CC is able to read the power consumption and RE generation readings directly from the meters, and is able to control power switching devices in all participating households.

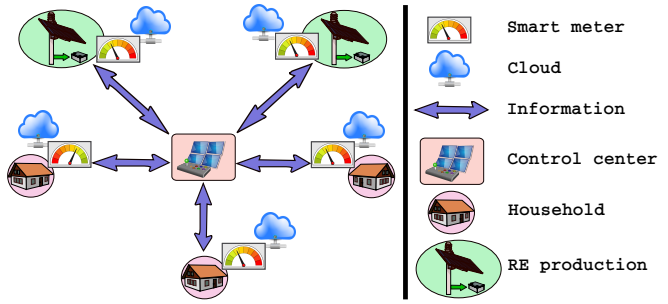

Fig. 2. Communication architechture for a shared-solar environment with $N = 2$ generation sites and $M = 3$ households. Biderctional arrows represent two-way information flows.

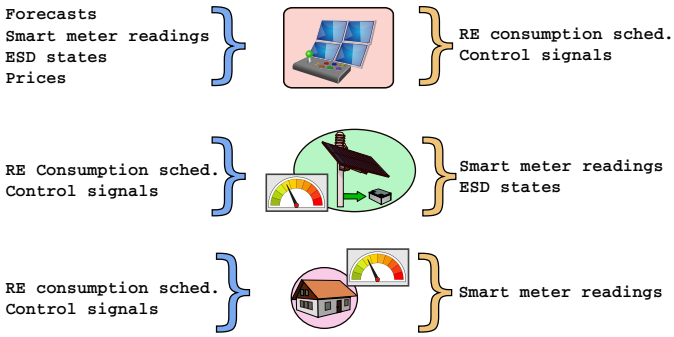

Fig. 3. Information flow requirements for a shared-solar environment. List of items on the left represents required inputs by each element of the system. List on the right represents outputting information.

The CC is in charge of the decision making throughout the planning period. As such, it receives real-time information from each household and RE production center. The information flows and the required infrastructure are shown in Figs. 2 and 3. The communication links shown in Fig. 2 do not necessarily represent connecting wires, as the information can be transmitted through the cloud.

As shown in Fig. 3, the CC requires the following information: 1) Forecasts: They are used to estimate the total RE production at each generation site over the planning period. They can be computed by using weather data and dedicated models. 2) Smart meter readings: This information comes from all the participating households and RE generation sites. They are used to assess the current load requirements and RE production. They can also be used to refine the forecasting models used to estimate future RE production and energy consumption. 3) ESD states: This information comes from the RE generation sites and is used to estimate the amount of RE currently available in the system, also, to prevent battery overflow or undesired full depletion. 4) Prices: In a demand response setting, this information comes from the utility company. In general, prices may be forecast from current market indicators and other relevant variables. In our framework, they are assumed known to the CC.

As shown in Fig. 3, the CC computes the RE consumption schedules and broadcasts the results to all the participating households and the RE production sites. Moreover, several control signals are issued by the CC to activate power switching mechanisms when necessary, prevent battery overflow or full depletion, and release relevant warnings to participating households.

Households agree to participate in the optimization scheme from the beginning of the planning period. To ensure their full collaboration, households are rewarded with a share of the cost savings. Different savings allocation criteria can be used. In this paper we explained a fairness-based criterion, which seeks to allocate cost savings in proportion to the share of ownership that each household has in the RE production infrastructure. This scheme is discussed in Sec. V.

Finally, by participating in the proposed cooperation scheme, households do not compromise their own comfort standards or energy bills. This result follows from the fact that the power consumed by each household (i.e., its load) is not subject to optimization. Therefore, ignoring capital investments, the energy bill incurred through cooperation is at most the same as the one incurred when the households refuse to cooperate.

III. Problem Statement

In this section we formulate the main optimization problem and discuss its properties. The formulated optimization problem seeks to minimize the total cost incurred by all the M participating households in $[0, S]$, while accounting for power transmission losses, battery inefficiencies, and energy generation across the N RE generation sites.

A. Decision Variables and Constraints

The decision variables are the discharging schedules $D_{m,n}(\tau)$ which will determine the optimal RE consumption patterns. There are thus two kinds of constraints involved in the optimization problem. The first set of constraints follows from the bounded storage capacity of the ESDs, which are denoted respectively by $\Psi_1,\ \Psi_2, \ldots, \Psi_N$, and the causality condition, according to which only RE readily available in the ESDs can be dispatched. These constraints can be compactly stated as follows:

$$J_n(0)+\int_0^{\tau}\left[\alpha_n R_n(x)-\frac{1}{\beta_n}\sum_{m=1}^{M} D_{m,n}(x)\right]dx \leq \Psi_n,\ \forall\,\tau,\ \forall\,n, \tag{6}$$

and

$$J_n(0)+\int_0^\tau \left[\alpha_n R_n(x) - \frac{1}{\beta_n}\sum_{m=1}^{M} D_{m,n}(x)\right] dx \geq 0,\ \forall\ \tau,\ \forall\ n. \tag{7}$$

Constraints (6) and (7) were obtained by using the definition of $J_n(\tau)$, presented in (3), and are introduced to ensure that all the $J_n(\tau)$'s are within the range $[0, \Psi_n]$. A second type of constraints arises when the distributed RE generation is exclusively used by the participating households, i.e., when no RE can be injected into the grid. These constraints can be formally written as follows:

$$\sum_{n=1}^{N}\left[D_{m,n}(\tau) - K_{m,n}\left(D_{m,n}(\tau)\right)^2\right] \leq L_m(\tau),\ \forall\ \tau,\ \forall\ m, \tag{8}$$

where the loss coefficient $K_{m,n} \triangleq \rho_{m,n}\mathsf{dis}_{m,n}\frac{1}{\mathsf{V}^2}$ has been introduced to simplify notation. As seen, the loss coefficient increases with the distance and the resistance of the connecting line, and decreases with the operational voltage.[4]

B. Problem Formulation and Characteristics

We formulate the following mathematical problem to optimize the discharging schedules across households and RE generation sites:

$$\text{P0:} \quad \min_{D_{m,n}(\tau),\ m\in\{1,\ldots,M\},\ n\in\{1,\ldots,N\},\ \tau\in[0,S]} \chi$$
$$\text{s.t.} \quad (4),\ (5),\ (6),\ (7),\ \text{and}\ (8).$$

P0 is a very challenging problem because of the following reasons: Its objective is not a function, but a sum of functionals. Its decision variables are not scalar or vectors, but trajectories (functions defined in continuous time). Equations (6), (7) and (8) represent an infinite number of constraints, which must hold in all the realizations of the stochastic processes $L_1(\tau), \ldots, L_M(\tau)$ and $R_1(\tau), \ldots, R_N(\tau)$.

C. Feasibility

P0 is infeasible when the $D_{m,n}(\tau)$'s are upper bounded in such a way that constraint (5) cannot hold. This will happen when the power consumed by the household is lower than the total production of RE in the network, i.e., when

$$\sum_{m=1}^{M}\int_0^S L_m(\tau)d\tau < \sum_{n=1}^{N}\alpha_n\beta_n\int_0^S R_n(\tau)d\tau,$$

or when the maximum discharging rate permitted is insufficient to allow the consumption of the RE generated in $[0, S]$ by any generator within the network, i.e., when

$$q_{D,n}S < \alpha_n\beta_n\int_0^S R_n(\tau)d\tau,\ n\ \in\ \{1,\ldots,N\}.$$

In practice, local RE generation is often insufficient to match the load. Hence, the above feasibility condition can be satisfied in many practical scenarios.

[4]A higher operational voltage leads to lower transmission currents.

IV. Proposed Solutions

In this section we propose two strategies to solve problem P0. The first approach uses quadratic programming and requires discretization in time. The second approach uses variational methods and provides a solution directly in continuous time. The second approach is introduced to reduce the computational complexity of the first strategy and obtain deeper insight into the solution. The two proposed methods are genie-aided, and hence, they can be used to benchmark suboptimal strategies, and to devise real-time RE management algorithms based on forecasts.

A. QP-REO Solution Strategy

We propose a method to solve P0 by using quadratic programming techniques. For tractability, we will introduce a discrete-time version of the model, and determine the optimal $D_{m,n}(\tau)$ at a finite number of points in $[0, S]$. After introducing discretization, we cast the problem as a quadratically-constrained quadratic programming problem.

1) Formulation in Discrete Time: We divide the planning horizon into $T-1$ subintervals, and sample the functions $P_m(\tau)$, $D_{m,n}(\tau)$, $L_m(\tau)$ and $R_n(\tau)$, $\forall\ m$, $\forall\ n$, at T equally-spaced points, e.g., $p_m(t) = P_m(t\Delta t)$. The vectors obtained after the sampling are denoted by $\mathbf{p}_m$, $\mathbf{d}_{m,n}, \boldsymbol{\ell}_m$, and $\mathbf{r}_n$, respectively. Let Δt denote the sampling interval, $t\ \in\ \{1,\ldots,T\}$ be the time index, and $\mathbf{x}\ \in\ \mathbb{R}^{MNT}$ denote the MNT variables to be optimized over the entire planning horizon stacked as follows: $\mathbf{x} = [\mathbf{x}_1, \mathbf{x}_2, \ldots, \mathbf{x}_M]^\intercal$, where $\mathbf{x}_m = [\mathbf{y}_{m,1}, \ldots, \mathbf{y}_{m,T}]$ and $\mathbf{y}_{m,t} = [D_{m,1}(t\Delta t), D_{m,2}(t\Delta t), \ldots, D_{m,N}(t\Delta t)]$.

We now simplify notation by introducing the following definition $\mathbf{k}_m = \mathbf{1}_T \otimes [K_{m,1}, K_{m,2}, \ldots, K_{m,N}]$. Then, the objective in P0 can be approximated by using a quadratic form as $\chi \approx \Delta t\,[\epsilon - \mathbf{1}_M\mathbf{P}\mathbf{x} + \mathbf{x}^\intercal\mathbf{Q}\mathbf{K}\mathbf{x}]$, for $\epsilon \in \mathbb{R}$, $\mathbf{P}\ \in\ \mathbb{R}^{M\times MNT}$, $\mathbf{Q},\ \mathbf{K}\ \in\ \mathbb{R}^{MNT\times MNT}$ presented in Appendix A.

Constraints (4), (6) and (7) imply that $\mathbf{x}$ must satisfy

$$\mathbf{M}_1\mathbf{x} \preceq \mathbf{v}_1,\quad \mathbf{M}_2\mathbf{x} \preceq \mathbf{v}_2,\quad \mathbf{M}_3\mathbf{x} \preceq \mathbf{v}_3, \tag{9}$$

for matrices $\mathbf{M}_1$, $\mathbf{M}_2$ and $\mathbf{M}_3$, and vectors $\mathbf{v}_1$, $\mathbf{v}_2$ and $\mathbf{v}_3$, which are derived from (4), (6) and (7) in Appendix B. Constraints (5) imply

$$\mathbf{M}_4\mathbf{x} = \mathbf{v}_4, \tag{10}$$

for matrix $\mathbf{M}_4$ and vector $\mathbf{v}_4$ derived accordingly in Appendix B. Constraints (8) imply that $\mathbf{x}$ must satisfy the following quadratic form

$$\mathbf{1}_M\mathbf{U}_{m,t}\mathbf{x} - \mathbf{x}^\intercal\mathbf{V}_{m,t}\mathbf{x} \leq L_m(t\Delta t),\ \forall\ m,\ \forall\ t, \tag{11}$$

for some matrices $\mathbf{U}_{m,t}$ and $\mathbf{V}_{m,t}$. Optimization problem P0 has a discrete-time domain counterpart formulated as follows:

$$\text{P1:} \quad \max_{\mathbf{x}}\ \mathbf{1}_M\mathbf{P}\mathbf{x} - \mathbf{x}^\intercal\mathbf{Q}\mathbf{K}\mathbf{x}$$
$$\text{s.t.} \quad (9),\ (10)\ \text{and}\ (11).$$

In P1 we have removed the first term, i.e., $\Delta t\sum_{m=1}^{M}\sum_{t=1}^{T} p_m(t)\ell_m(t)$, because it does not depend on the design variable $\mathbf{x}$. Similarly, the constant Δt has

been omitted from the objective function for simplicity, as removing it does not affect the result of the optimization.

Remark 1: P1 is a quadratically-constrained quadratic programming problem in which we want to maximize a concave function of $\mathbf{x}$. P1 is not a convex optimization problem because the matrices $\mathbf{V}_{m,t}$ are positive definite and preceded by a negative sign in constraints (11). To show that $\mathbf{V}_{m,t}$ is a positive definite matrix, we note that it is a diagonal matrix, since no cross-terms appear in (11), and all its elements are non-negative because the coefficients of the quadratic terms $[D_{m,n}(\tau)]^2$ are all positive, i.e., the resistance per unit length $\rho_{m,n}$, the distance between the generators and the households $\mathsf{dis}_{m,n}$, and the voltage V, are all non-negative.

2) Convex Relaxation: To tackle P0, we propose to substitute constraints (11) with

$$\mathbf{1}_M \mathbf{U}_{m,t}\mathbf{x} \leq L_m(t\Delta t),\ \forall\ m,\ \forall\ t. \tag{12}$$

Note that the solution obtained by enforcing (12) will satisfy the original constraint (11) because (12) is more stringent than the original constraint. The relaxed optimization problem is convex because it is formulated to maximize a concave objective and all its constraints are affine. Hence, this problem can be solved by using existing techniques to tackle quadratic programming problems [42].

The performance loss incurred as a result of introducing the relaxed constraint (12) instead of (11) can be assessed in the following manner. P1 can be solved without constraint (11) as an ordinary quadratic programming problem with no quadratic constraints. The result obtained will be a performance upper bound for the original problem P1, since it has a larger feasible space, which allows for a wider search. That is, the solution obtained after removing constraint (11) is at least, as good as the solution to the original problem. On the other hand, the solution obtained when (12) is accounted for in the problem is at most as good as the solution of the original problem. This follows because replacing (11) with (12) constrains the feasible space further. Given that the feasible space of the original problem is smaller than the feasible space obtained after removing (11), but larger than the search space that results after introducing (12), we can say that the performance loss incurred by this relaxation is at most, as large as the gap between the solutions obtained with and without constraint (12). In formal language:

Let P1a denote the proposed relaxed version of P1, and P1b denote P1 without constraint (12), that is:

$$\begin{aligned} \text{P1a:}\quad & \max_{\mathbf{x}}\ \ \mathbf{1}_M\mathbf{P}\mathbf{x} - \mathbf{x}^\intercal\mathbf{Q}\mathbf{K}\mathbf{x} \\ \text{s.t.}\quad & \text{(9), (10) and (12),} \end{aligned}$$

and

$$\begin{aligned} \text{P1b:}\quad & \max_{\mathbf{x}}\ \ \mathbf{1}_M\mathbf{P}\mathbf{x} - \mathbf{x}^\intercal\mathbf{Q}\mathbf{K}\mathbf{x} \\ \text{s.t.}\quad & \text{(9) and (10).} \end{aligned}$$

Moreover, let $\mathsf{sol}(P)$ denote the solution to a maximization problem denoted by P. Then, for P1a, P1 and P1b, as defined above, it follows that:

$$\mathsf{sol}(\text{P1a}) \leq \mathsf{sol}(\text{P1}) \leq \mathsf{sol}(\text{P1b}). \tag{13}$$

Following (13), we can bound the solution to P1 by solving P1a and P1b. This inequality will allow us to assess the quality of the solution found through relaxation.

B. CoV-REO Solution Strategy

In the following we propose a solution based on variational methods. We will first introduce reasonable simplifications to the optimization problem. Then we will apply the Euler-Lagrange optimality condition to find candidate solutions, which we will adjust to comply with required constraints. Finally, we will analyze the solution and determine its application range.

1) Simplifications: When the discharging rates across the ESDs in the system are unrestricted, the existence of a feasible solution is guaranteed. Studying such a case allows us to: 1) Find a closed-form solution. 2) Obtain valuable insights, which are not provided by the solution based on quadratic programming. 3) Simplify online algorithms based on model predictive control, given that decision variables can be updated faster than when using quadratic programming.

2) Euler-Lagrange Optimality Condition: To obtain a solution based on CoV, we first consider the objective function in P0, and determine the conditions under which the functionals in (2) are stationary. We start by introducing the following notation: Let Θ_n be the total RE delivered by the nth generator in $[0, S]$. Then, following constraint (5), the decision variables $D_{m,n}(\tau)$ must satisfy:

$$\sum_{m=1}^{M}\int_0^S D_{m,n}(\tau)d\tau = \Theta_n,\ \forall\ n. \tag{14}$$

Thus, by introducing the artificial constraint written above, we can write the Euler-Lagrange equations [43], which will allow us to establish the necessary conditions for the $D_{m,n}(\tau)$'s to minimize the sum of functionals in (2):

$$\frac{\partial}{\partial D_{m,n}}\left[\chi + \lambda_n\left[\sum_{m=1}^{M}\int_0^S D_{m,n}(\tau)d\tau - \Theta_n\right]\right] = 0,\ \forall\ n, \tag{15}$$

where $\lambda_n \in \mathbb{R}_{\geq 0}$ are the Lagrange multipliers. The condition (15) leads to:

$$-P_m(\tau) + 2\rho_{m,n}\mathsf{dis}_{m,n}\frac{D_{m,n}(\tau)}{\mathsf{V}^2}P_m(\tau) + \lambda_n = 0,\ \forall\ n. \tag{16}$$

Hence, the optimal $D_{m,n}(\tau)$ should satisfy:

$$D_{m,n}(\tau) = \frac{1}{2K_{m,n}}\left[1 - \frac{\lambda_n}{P_m(\tau)}\right]. \tag{17}$$

3) Constraints Satisfaction: The constants λ_n's in (17) can be chosen to comply with the artificial constraint (14). Specifically, after substituting (17) in (14), we obtain:

$$\lambda_n = \frac{\sum_{m=1}^{M}\frac{S}{2K_{m,n}} - \Theta_n}{\sum_{m=1}^{M}\frac{1}{2K_{m,n}}\int_0^S \frac{1}{P_m(\tau)}d\tau},\ \forall\ n. \tag{18}$$

To satisfy constraint (5), we set $\Theta_n = \alpha_n\beta_n\int_0^S R_n(\tau)d\tau$, and to comply[5] with constraint (7) we set $J_n(0) = \Theta_n,\ \forall\ n$. Finally, constraint (6) is satisfied when $\Psi_n \geq 2\Theta_n$, which will ensure that $J_n(\tau) \leq \Psi_n,\ \forall\ \tau,\ \forall\ n$.

[5]This can be shown by using the principle of conservation of energy.

4) Concavity of the Cost Savings Function: By replacing the obtained schedules in the objective function χ, we can investigate the relationship between the energy cost and the total RE delivered by each generation site, denoted by Θ_n. To simplify notation, we introduce the following definition

$$\xi \triangleq \sum_{m=1}^{M} \int_0^S P_m(\tau) L_m(\tau) d\tau - \chi, \tag{19}$$

which can be interpreted as the cost savings obtained through RE management. Note that if $R_n(\tau) = 0,\ \forall\ \tau,\ \forall\ n$, then $\xi = 0$, and the energy cost incurred by the M households is simply $\sum_{m=1}^{M} \int_0^S P_m(\tau) L_m(\tau) d\tau$.

The cost saving ξ is a function of the Θ_n's, hence, we can write this explicitly by using the notation $\xi\left[\Theta_1, \ldots, \Theta_N\right]$. Moreover, we can make the following claim regarding the concavity of the cost function $\xi\left[\Theta_1, \ldots, \Theta_N\right]$ with respect to each of the Θ_n's:

Theorem 1. *Let* $D^*_{m,n}(\tau) = \frac{1}{2K_{m,n}}\left[1 - \frac{\lambda_n}{P_m(\tau)}\right]$ *with* $\lambda_n = \frac{\sum_{m=1}^{M} \frac{S}{2K_{m,n}} - \Theta_n}{\sum_{m=1}^{M} \frac{1}{2K_{m,n}} \int_0^S \frac{1}{P_m(\tau)} d\tau}$, $K_{m,n} > 0,\ \forall\ m \in \{1, \ldots, M\},\ n \in \{1, \ldots, N\}$. *If* $D_{m,n}(\tau) = D^*_{m,n}(\tau),\ \forall\, m,\ \forall\, n,\ \forall\, \tau$, *then,* ξ, *as defined in* (19) *is concave in* $\Theta_n,\ \forall\ n$.

Proof. See Appendix C. ∎

Corollary 1. *Since* $\xi\left[\lambda_1(\Theta_1), \ldots, \lambda_N(\Theta_N)\right]$ *is concave in* Θ_n, *it attains its maximum at*

$$\Theta_n = \Theta^*_n \triangleq \frac{S}{2} \sum_{m=1}^{M} \frac{1}{K_{m,n}},\ \forall\ n. \tag{20}$$

Proof. To obtain this result we set $\frac{\partial}{\partial \lambda_n} \xi = 0$, which in turn implies that $\lambda_n = 0,\ \forall\ n$. Hence, from (18) we obtain $\Theta_n = \frac{S}{2} \sum_{m=1}^{M} \frac{1}{K_{m,n}}$. ∎

Remark 2: Following Theorem 1, if the optimal RE consumption schedules satisfy (17), then the optimal RE generation at each site is directly proportional to the length of the planning horizon S, and the sum $\sum_{m=1}^{M} \frac{1}{K_{m,n}}$. When $\Theta_n > \Theta^*_n$ the value of ξ is less than or equal to the value of ξ when $\Theta_n = \Theta^*_n$. This result follows because larger discharging rates incur higher transportation losses thus making them suboptimal. Interestingly, the turning point is determined by the length of the planning horizon and characteristics of the line such as resistance and length. Specifically, the smaller the resistance is, i.e., the product $\rho_{m,n}\mathsf{dis}_{m,n}$, the farther is the stationary point. The stationary point increases with the transmission voltage V.

Remark 3: The optimal RE generation at the nth site, and denoted by Θ^*_n, specifies the largest amount of energy that the site can deliver, before power transmission losses significantly undermine the optimization gain. We can thus use Θ^*_n to determine an upper bound in the RE production capacity and the required size of the ESD at each generation site.

5) Range of Applicability: The result in (17) is applied when $\left[1 - \frac{\lambda_n}{P_m(\tau)}\right] \geq 0$, which implies

$$\Theta_n \geq \sum_{j=1}^{M} \frac{S}{2K_{j,n}} - \min_{m,t}\left[P_m(\tau) \sum_{j=1}^{M} \frac{1}{2K_{j,n}} \int_0^S \frac{1}{P_j(\tau)} d\tau\right]. \tag{21}$$

Moreover, given that $\lambda_n \geq 0,\ \forall\ n$, we have:

$$\Theta_n \leq \frac{S}{2} \sum_{m=1}^{M} \frac{1}{K_{m,n}}. \tag{22}$$

These two inequalities determine the range of applicability of the proposed CoV-REO strategy.

C. Complexity Analysis of the Proposed Strategies

In this section we discuss the time and space complexity of the QP-REO and the CoV-REO strategies.

1) Time Complexity: We first investigate the number of mathematical operations that are needed in CoV-REO. A breakdown of these operations is shown in Tables I and II. As seen, the total number of operations needed in CoV-REO is $3MNT + 3MN + 4N + M$. If each of these operations can be completed in constant time, then the time complexity of CoV-REO scales up linearly with T, the number of samples considered in the planning horizon.

The arithmetic cost of solving quadratically-constrained quadratic programming (QCQP) problems has been investigated in [44], where the authors showed that path-following methods can reach a solution within $O(1)(\mathsf{mn}^2 + \mathsf{n}^3)$ operations, where $O(1)$ represents absolute constant, m is the number of quadratic constraints, and n is the size of the matrices used to express the quadratic forms in both constraints and objective function. For the specific case of P1, and after the convex relaxation of Sec. IV-A-2, we have $\mathsf{m} = 0$, and

TABLE I
OPERATIONS REQUIRED TO COMPUTE $D_{m,n}(t\Delta t)$ IN EACH $t \in \{1, \ldots, T\}$, AND $\forall\, m,\ \forall\, n$.

Operation	Description	Quantity
$\frac{\lambda_n}{P_m(t\Delta t)}$	Division	MN
$1 - \frac{\lambda_n}{P_m(t\Delta t)}$	Subtraction	MN
$\frac{1}{2K_{m,n}}\left[1 - \frac{\lambda_n}{P_m(\tau)}\right]$	Multiplication	MN

TABLE II
OPERATIONS REQUIRED TO COMPUTE THE λ_n'S.

Operation	Description	Quantity
$\sum_0^T \frac{1}{P_m(t\Delta t)} \Delta t$	Integration	M
$\frac{1}{2K_{m,n}}$	Division	MN
$\frac{1}{2K_{m,n}} \sum_0^T \frac{1}{P_m(t\Delta t)} \Delta t$	Multiplication	MN
$\sum_{m=1}^{M} \frac{1}{2K_{m,n}} \sum_0^T \frac{1}{P_m(t\Delta t)} \Delta t$	Sum	N
$\frac{S}{2K_{m,n}}$	Division	MN
$\sum_{m=1}^{M} \frac{S}{2K_{m,n}}$	Sum	N
$\sum_{m=1}^{M} \frac{S}{2K_{m,n}} - \Theta_n$	Subtraction	N
$\frac{\sum_{m=1}^{M} \frac{S}{2K_{m,n}} - \Theta_n}{\sum_{m=1}^{M} \frac{1}{2K_{m,n}} \sum_0^T \frac{1}{P_m(t\Delta t)} \Delta t}$	Division	N

$\mathsf{n} = MNT$. Hence, the number of operations required to solve P1 in its relaxed form scales up with $M^3N^3T^3$. As seen, both strategies are able to obtain a solution in polynomial time. However, the strategy based on calculus of variations is faster, as the number of operations is a multiple of MNT, and not $M^3N^3T^3$, as in the case of QP-REO.

2) Space Complexity: In terms of memory requirements, both QP-REO and CoV-REO are similar, since they both rely on the same amount of information. The memory space requirements in both strategies are expected to grow linearly with the number of samples in the planning period. This can be seen from the sizes of the vector $\mathbf{x}$ and the matrices $\mathbf{P}$, $\mathbf{Q}$ and $\mathbf{K}$. Memory release may be more efficient in the CoV-REO strategy, given that the decision variables can be updated one sample at a time. This also allows us to use this strategy in a faster way for computing decision variables in real time, e.g., in response to changing conditions and updated forecasts.

V. Energy Allocation Policy and Ownership Distribution

In this section we propose strategies to ensure the full cooperation of the participating households. The first strategy is a fair energy allocation policy, which seeks to limit the amount of RE used by each household, in proportion to its contribution towards infrastructure investment. In this strategy the ownership distribution is fixed. The second strategy seeks to establish the optimal ownership distribution so as to minimize the energy cost incurred by all the participating households, while ensuring a fair energy allocation. By using the second strategy, we show how the optimal ownership distribution is determined by the electricity prices, the RE production capacity of each generation site, and the characteristics of the transmission lines connecting generators and households.

A. Fair Energy Allocation Policy

To ensure full cooperation among the participating households we now derive a fairness-maximizing energy allocation policy. The proposed energy allocation policy complements the result derived in Sec. IV-B, and ensures that each household uses a share of RE which is proportional to its initial investment in any given generation site. Let $0 \leq \gamma_{m,n} \leq 1$ denote the share of ownership that household m has of the nth RE generation site. Since all the participating households collectively own each of the RE generation sites, the $\gamma_{m,n}$'s satisfy $\sum_{m=1}^{M} \gamma_{m,n} = 1,\ \forall\ n$.

To ensure that each household uses a fraction $\gamma_{m,n}$ of the energy generated by the nth RE generation site, we add the following set of constraints to the original optimization problem (P0):

$$\int_0^S D_{m,n}(\tau)d\tau = \gamma_{m,n}\alpha_n\beta_n \int_0^S R_n(\tau)d\tau,\ \forall\ n. \tag{23}$$

Hence, the optimization problem becomes:

$$\text{P2:} \quad \min_{D_{m,n}(\tau),\ m\in\{1,\ldots,M\},\ n\in\{1,\ldots,N\},\ \tau\in[0,S]} \ \chi$$
$$\text{s.t.} \quad (4),\ (5),\ (6),\ (7),\ (8),\ \text{and}\ (23).$$

The added constraints are all affine, and hence, they can be handled by using both, the QP-REO and the CoV-REO strategies. However, adding these constraints may render the problem infeasible when:

$$\int_0^S L_m(\tau)d\tau < \sum_{n=1}^{N} \gamma_{m,n} \int_0^S R_n(\tau)d\tau, \tag{24}$$

for any $m \in \{1,\ldots,M\}$. The condition (24) refers to situations in which the RE assigned to any household is above its load requirement in $[0, S]$. If the conditions explained in Sec. IV-B hold, then we can use the result (17) to determine the solution to P2 as follows:

$$D_{m,n}(\tau) = D'_{m,n}(\tau) \triangleq \frac{1}{2K_{m,n}}\left[1 - \frac{\lambda'_{m,n}}{P_m(\tau)}\right],\ \forall\ \tau, \tag{25}$$

where $\lambda'_{m,n} \in \mathbb{R}$ can be obtained by substituting (25) in (23), yielding:

$$\lambda'_{m,n} = \frac{\frac{1}{2K_{m,n}}S - \gamma_{m,n}\alpha_n\beta_n \int_0^S R_n(\tau)d\tau}{\frac{1}{2K_{m,n}}\int_0^S \frac{1}{P_m(\tau)}d\tau},\ \forall\ n. \tag{26}$$

This solution applies when the RE produced by the nth generator satisfies

$$\int_0^S R_n(\tau)d\tau \leq \min_m \frac{1}{2\alpha_n\beta_n K_{m,n}\gamma_{m,n}}S. \tag{27}$$

Similarly, the solution (25) is applied when $\lambda'_{m,n} < P_m(\tau),\ \forall\ m,\ t$, which implies

$$\int_0^S R_n(\tau)d\tau \geq \max_{m,t} \frac{1}{2\alpha_n\beta_n K_{m,n}\gamma_{m,n}}\left[S - P_m(\tau)\int_0^S \frac{1}{P_m(\tau)}d\tau\right]. \tag{28}$$

B. Optimal Ownership Distribution

Imposing the added constraints (23) will result in performance degradation. Hence, we now want to know what are the values of $\gamma_{m,n}$ that minimize such a performance loss. The set of $\gamma_{m,n}$ values determine the ownership distribution across households of each RE generator in the system. To minimize the performance degradation incurred after introducing constraints (23) we now formulate a mathematical problem to choose the optimal share of ownership across households, i.e., the values of $\gamma_{m,n}$.

1) Problem Formulation: The mathematical problem which seeks to optimize RE consumption schedules, RE allocation policy, and ownership distribution is:

$$\text{P3:} \quad \min_{D_{m,n}(\tau),\ \gamma_{m,n},\ m\in\{1,\ldots,M\},\ n\in\{1,\ldots,N\},\ \tau\in[0,S]} \ \chi$$
$$\text{s.t.} \quad (4),\ (5),\ (6),\ (7),\ (8),\ (23),\ \text{and}\ \sum_{m=1}^{M} \gamma_{m,n} = 1,\ \forall\ n.$$

2) Solution Approach: P3 is a very challenging optimization problem and, to the best of our knowledge, cannot be tackled directly. Hence, we propose breaking P3 into two subproblems. A natural decomposition is thus to initially determine the optimal RE consumption schedules and the allocation policy, and then choose the ownership distribution so as to minimize the performance degradation. The first subproblem can be tackled by using either the QP-REO or the CoV-REO strategy. A solution to the second subproblem can be worked out from the optimal RE consumption schedules. Indeed, an insightful solution can be derived if results in closed form are available from the first stage, as we show in Sec. V-B3.

Let $D^*_{m,n}(\tau)$ denote the optimal RE consumption schedules, obtained by solving P0. Then, the ownership ratios that minimize the collective energy cost and ensure full cooperation across households are given by:

$$\gamma^*_{m,n} = \frac{\int_0^S D^*_{m,n}(\tau)d\tau}{\Theta_n}. \tag{29}$$

3) Special Cases: If the conditions explained in Sec. IV-B hold, then a more insightful solution can be obtained by using the results (17) and (18). Specifically, replacing (17) in (29) yields:

$$\gamma^*_{m,n} = \frac{1}{2K_{m,n}\Theta_n}\left[S - \lambda_n \int_0^S \frac{1}{P_m(\tau)}d\tau\right]. \tag{30}$$

By replacing (18) into (30), it can easily be shown that $\sum_{m=1}^{M} \gamma^*_{m,n} = 1$. Moreover, following Corollary 1, the optimal ownership distribution is:

$$\gamma^*_{m,n} = \frac{\frac{1}{K_{m,n}}}{\sum_{j=1}^{M} \frac{1}{K_{j,n}}}. \tag{31}$$

The ownership distribution stated in (30) does not depend on the energy consumed by each household because $L_m(\tau)$ is large, and hence unable to restrict the RE consumption schedules. The investment allocation given in (30) depends on the RE generation capacity of each site, the electricity prices offered to each household, and the characteristics of the transmission lines connecting households and generators. Implementing this ownership distribution thus involves rebalancing the investment allocation at the start of each planning period.

Contrarily, the optimal ownership distribution stated in (31) depends on the characteristics of the transmission lines connecting households and generators. To implement this ownership allocation all the RE generation sites should deliver exactly Θ^*_n energy units. When $\Theta_n = \Theta^*_n,\ \forall\ n$, the transmission losses dominate the RE allocation and consumption policies, thus making the pricing functions $P_m(\tau)$ irrelevant.

VI. Numerical Results

We provide numerical results to analyze the proposed strategies. Several simulation scenarios (load, RE generation profiles and prices) are considered in this section in order to illustrate the characteristics of the proposed strategies. We divide this section into five parts. In the first part we investigate the characteristics of the solution based on quadratic programming. The quadratic programming problems are solved by using CVX on Matlab. In the second part we compare the solution obtained with the variational method and the conventional quadratic programming approach. In the third part we verify the analysis presented in Sec. V, regarding the energy allocation policy and the ownership distribution. In the fourth part we present a practical case with real life parameters. Finally, we provide additional simulations and consider other cases in part five.

In sections VI-A, VI-B, VI-C, and VI-E, storage capacity is measured in energy units [EU], and energy expenditure in monetary units [MU]. Similarly, time, power, and electric potential are measured in time units [TU], power units [PU], and electric potential units [EPU]. In these sections we use generic measurement units because we want to verify the analytical results presented in the paper by comparing them against numerical solutions in arbitrary simulation scenarios. Moreover, the numerical results need to be interpreted in relative terms, as they illustrate the performance gap between the proposed strategies under the same scenario.

To simplify notation, in this section we will use $D_m(\tau)$ to denote the total renewable power drawn by the mth household at time τ, i.e., $D_m(\tau) = \sum_{n=1}^{N} D_{m,n}(\tau),\ \forall\ \tau$. Moreover, to avoid repetition, the system parameters that are consistent throughout sections VI-A, VI-B, VI-C, and VI-E, are presented in Table III.

TABLE III
System Parameters

Parameter	Value
$\{T,\ \Delta t,\ M,\ N,\ \mathsf{V}\}$	$\{20[\mathsf{TU}],\ 1[\mathsf{TU}],\ 3,\ 2,\ 1[\mathsf{EPU}]\}$
$q_{D,n}$	$\Delta t \sum_{t=1}^{T} r_n(t)[PU],\ \forall\ n$
$\{\alpha_n,\ \beta_n,\ \Psi_n,\ J_n(0)\}$	$\{1,\ 1,\ \Delta t \sum_{t=1}^{T} r_n(t)[\mathsf{EU}],\ 0,\ \forall\ n\}$

A. Solution based on Quadratic Programming

We start by illustrating the characteristics of the RE consumption schedule. We thus consider time-varying electricity prices and loads, and fixed resistances across connecting lines of equal length. Specifically, we consider the price and load profiles illustrated in Fig. 4, and let $K_{1,1} = K_{1,2} = 0.01$, $K_{2,1} = K_{2,2} = 0.01$, and $K_{3,1} = K_{3,2} = 0.01$. In Fig. 4 we can see that, when the lines connecting the households and the RE generators have the same characteristics (length and resistance), the RE consumption rate is influenced by the price variations across time, and the loads. When the load is above the RE generation at all times, then the optimal schedule responds to price variations across time. When the load is below the RE generation at all times, then the optimal schedule is determined by the loads, since the consumption of RE is upper bounded by the load in each household.

We now investigate the effect of the power loss factor in the RE consumption pattern. We thus consider constant prices, loads and RE generation profiles, but varying distances and line resistances. Specifically, we consider the price, load and RE generation profiles illustrated in Fig. 5, and

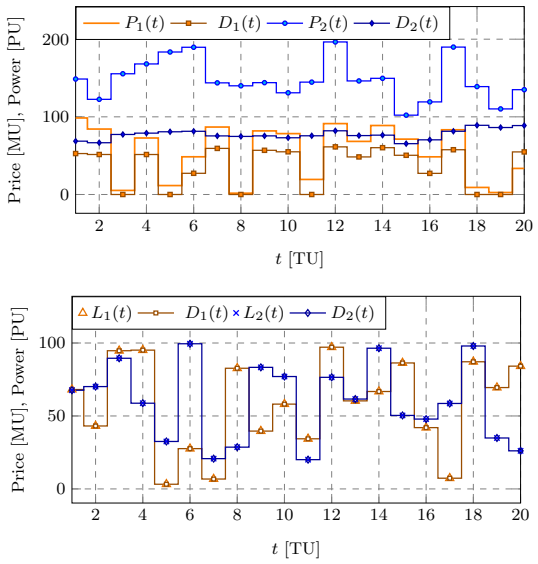

Fig. 4. Time-variation of RE consumption rate. Top: Influenced by price. Bottom: Influenced by the load.

let $K_{1,1} = K_{1,2} = 0.005$, $K_{2,1} = K_{2,2} = 0.008$, and $K_{3,1} = K_{3,2} = 0.01$. In Fig. 5 we illustrate both, the RE consumption rates across time, and the result of the RE allocation strategy. As seen, the RE consumption rates are nearly constant. The variations across time are of 0.1% at most, and follow inaccuracies produced by the employed numerical Software. Since $K_{m,1} = K_{m,2}$, $\forall\, m$, in this scenario the share of RE that goes to the mth household from the nth generator is given by the ratio $\frac{\frac{1}{K_{m,n}}}{\sum_{j=1}^{M}\frac{1}{K_{j,n}}}$.

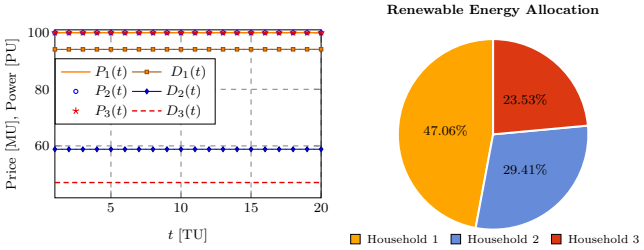

Fig. 5. Effect of power loss in RE allocation across households. The share of RE allocated to each household is given by $\frac{\frac{1}{K_{m,n}}}{\sum_{j=1}^{M}\frac{1}{K_{j,n}}}$.

When the power loss is high, e.g., when $K_{11} = K_{12} = K_{21} = K_{22} = K_{31} = K_{32} = 0.02$, prices will have a diminished impact on the RE allocation policy. As seen in Fig. 6, all households get the same share of RE use, despite the price differences across locations. This result follows because the load is above the RE generation at all times, the lines connecting households and RE generators have the same characteristics (length and resistance), and the quadratic term dominates the objective function in P0.

As expected, prices will dominate the RE allocation policy when households and RE generators have similar characteristics, and when the power loss is not as dominant as in the scenario considered in Fig. 6. This can be seen in Fig. 7, where we considered a scenario in which prices vary across locations and connecting lines offer less than significant resistance, i.e., $K_{11} = K_{12} = K_{21} = K_{22} = K_{31} = K_{32} = 0.002$.

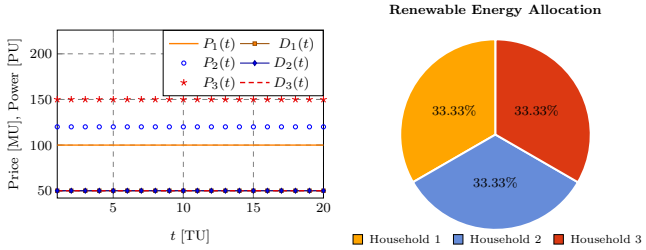

Fig. 6. Power loss dominates RE allocation across households. $K_{11} = K_{12} = K_{21} = K_{22} = K_{31} = K_{32} = 0.02$. The share of RE allocated to each household is given by $\frac{\frac{1}{K_{m,n}}}{\sum_{j=1}^{M}\frac{1}{K_{j,n}}}$.

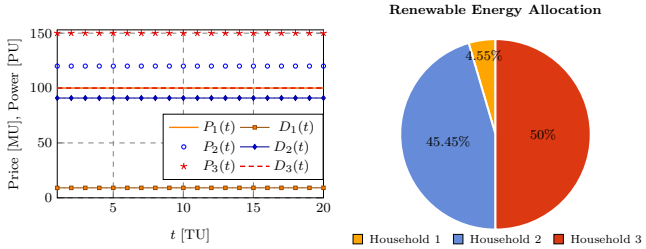

Fig. 7. Price dominates RE allocation across households. $K_{11} = K_{12} = K_{21} = K_{22} = K_{31} = K_{32} = 0.002$.

B. Solution based on Variational Methods and Comparison

In this section we compare the solutions obtained with the quadratic programming approach and the variational method. For simplicity, we consider 30 samples over the normalized time scale $[0, 1]$. We consider four simulation scenarios as follows:

- Scenario 1: $P_1(\tau) = \sin(7\tau) + 2$, $P_2(\tau) = \cos(7\tau) + 2$, $P_3(\tau) = \sin(8\tau) + 2$, $K_{1,1} = 0.05$, $K_{1,2} = 0.06$, $K_{2,1} = 0.07$, $K_{2,2} = 0.08$, $K_{3,1} = 0.09$, $K_{3,2} = 0.1$.
- Scenario 2: $P_1(\tau) = \sin(7\tau) + 2$, $P_2(\tau) = \cos(7\tau) + 2$, $P_3(\tau) = \sin(8\tau) + 2$, $K_{1,1} = 0.0471$, $K_{1,2} = 0.0561$, $K_{2,1} = 0.0269$, $K_{2,2} = 0.0749$, $K_{3,1} = 0.0504$ $K_{3,2} = 0.0647$.
- Scenario 3: $P_1(\tau) = \sin(10\tau) + 2$, $P_2(\tau) = \cos(5\tau) + 2$, $P_3(\tau) = \sin(18\tau) + 2$, $K_{1,1} = 0.0904$, $K_{1,2} = 0.0667$, $K_{2,1} = 0.0118$, $K_{2,2} = 0.1482$, $K_{3,1} = 0.1014$ $K_{3,2} = 0.04$.
- Scenario 4: $P_1(\tau) = \sin(10\tau) + 2$, $P_2(\tau) = \cos(5\tau) + 2$, $P_3(\tau) = \sin(18\tau) + 2$, $K_{1,1} = 0.144$, $K_{1,2} = 0.0694$, $K_{2,1} = 0.1034$, $K_{2,2} = 0.1113$, $K_{3,1} = 0.0313$ $K_{3,2} = 0.1124$.

In all these scenarios, $M = 3$, $N = 2$, $S = 1$, $T = 30$, $\Delta t = 0.0345$, and the battery parameters are set as in Table III, except for the $J_n(0)$'s which are set according to the requirements stated in Sec. IV-B, i.e., $J_n(0) = \int_0^S R_n(\tau)d\tau$, $\forall\, n$.

As seen in Fig. 8, the strategy based on calculus of variations is able to approximate the result obtained through quadratic programming whenever $\frac{\lambda_n}{P_m(\tau)} < 1,\ \forall\ m,\ \forall\ n$. That is, whenever the conditions considered in Sec. IV-B hold, the result (17) is close to the one obtained numerically through quadratic programming.

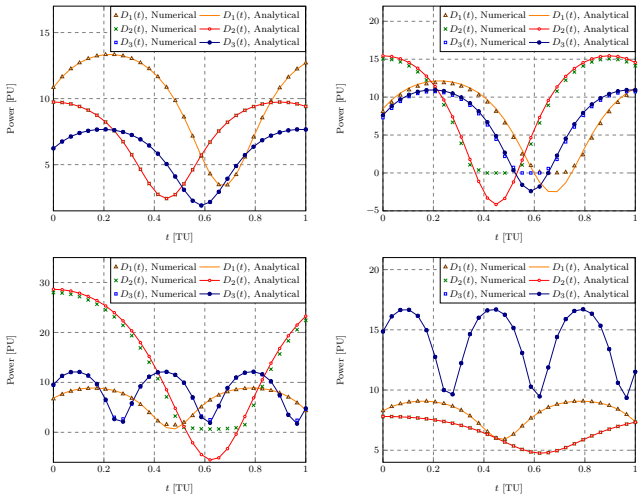

Fig. 8. Time-variation of RE consumption rate. Top-Left: Scenario 1. Top-Right: Scenario 2. Bottom-Left: Scenario 3. Bottom-Right: Scenario 4.

We now compare the performance of the proposed strategies in terms of achievable cost savings. In Fig. 9, we plot ξ against Θ_1 while setting Θ_2 to half its optimal value, according to (20), in each of the simulation scenarios described above. As seen, the cost saving function is concave in Θ_1 and attains its maximum when $\Theta_1 = \frac{S}{2}\sum_{m=1}^{M}\frac{1}{K_{m,n}}$, according to (20). Similarly, in Fig. 10, we plot ξ against Θ_2 while letting $\Theta_1 = \Theta_1^*$, where Θ_1^* is given by (20). Again, we consider the four simulation scenarios described above. Figs. 10 verify the fact that the cost saving function is concave in Θ_2 and attains its maximum when $\Theta_2 = \frac{S}{2}\sum_{m=1}^{M}\frac{1}{K_{m,n}}$, according to (20). The performance gap shown in Figs. 9 and 10 for small and large values of Θ_1 and Θ_2 follows from the range of applicability determined in Sec. IV-B5.

C. Ownership Distribution

We now verify some of the results presented in Sec. V. We thus consider the simulation scenarios described in Sec. VI-B, as well as varying ownership shares of the first and second households, while we set the ownership share of the third household to its optimal value. That is, we set $\gamma_{1,2} = \gamma_{1,2}^*$, $\gamma_{2,2} = \gamma_{2,2}^*$, $\gamma_{3,1} = \gamma_{3,1}^*$, $\gamma_{3,2} = \gamma_{3,2}^*$, and let $\gamma_{1,1}$ vary between 0 and $1-\gamma_{3,1}^*$ and $\gamma_{2,1}$ vary between 0 and $1-\gamma_{1,1}-\gamma_{3,1}^*$. Then, we plot the achievable cost savings ξ against $\gamma_{1,1}$ in Fig. 11 for the four simulation scenarios described in Sec. VI-B. The optimal value of $\gamma_{1,1}$, computed by using (30), is marked in the plots. As observed, the cost savings function ξ is concave in $\gamma_{1,1}$, and the expression (30) is able to estimate its optimized value within reasonable accuracy.

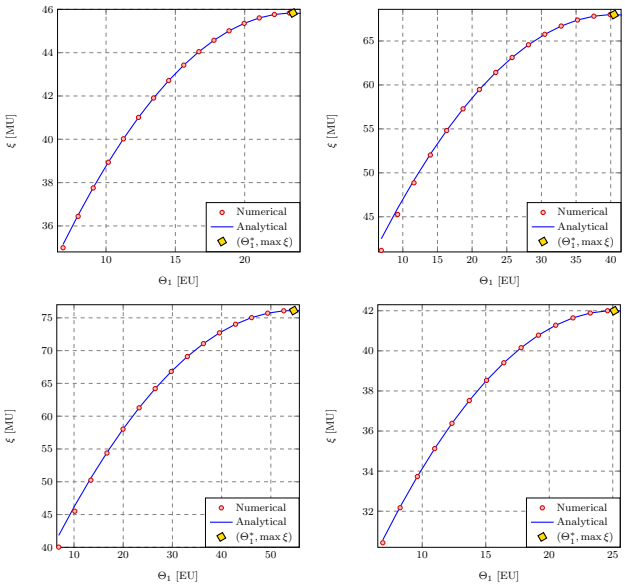

Fig. 9. Comparative performance: QP-REO vs. CoV-REO. Cost savings plotted against RE production at first generation site. Top-Left: Scenario 1. Top-Right: Scenario 2. Bottom-Left: Scenario 3. Bottom-Right: Scenario 4.

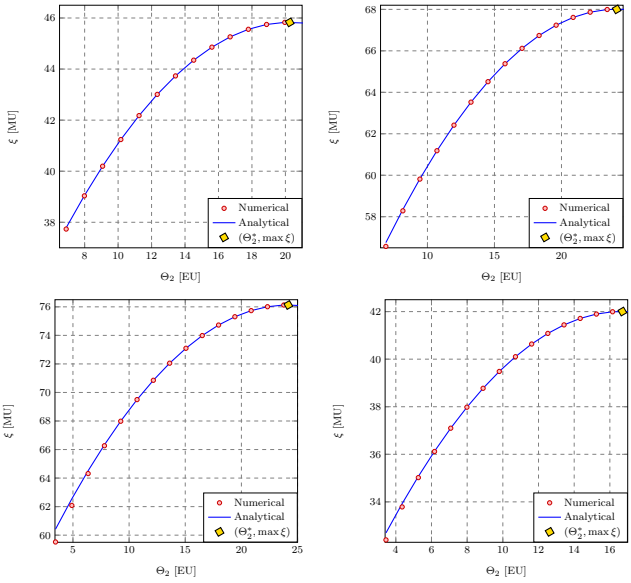

Fig. 10. Comparative performance: QP-REO vs. CoV-REO. Cost savings plotted against RE production at second generation site. Top-Left: Scenario 1. Top-Right: Scenario 2. Bottom-Left: Scenario 3. Bottom-Right: Scenario 4.

D. Practical Case

We consider two RE generation sites, each with 10 solar panels and a maximum output power of 320[W] per panel, as described in [45]. Each generation site is equipped with a battery bank composed of 6 lead acid batteries, each with a capacity of 210[Ah] and an operating voltage of 12[V], as described in [46]. We consider two simulation scenarios: In the first scenario, 3 houses are located 443.07 metres from each generation site. In the second simulation scenario, the three houses are located 553,84 metres from each generation site. In

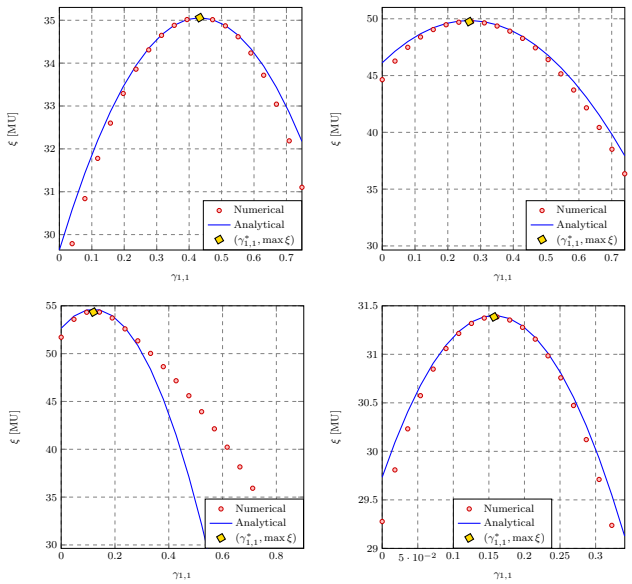

Fig. 11. Comparative performance: QP-REO vs. CoV-REO. Cost savings plotted against household one's ownership share of first generation site. Top-Left: Scenario 1. Top-Right: Scenario 2. Bottom-Left: Scenario 3. Bottom-Right: Scenario 4.

both scenarios, we assume connecting wires with a resistance of 1.3mΩ per meter, which corresponds to AWG 6 [47]. Moreover, in both scenarios the households are subject to the same real-time energy prices offered by Southern California Edison to its medium-size customers on a hot summer day [48]. In both scenarios, we consider a 24-hour long planning period, and initialize the battery bank at generation site 1 as $\Theta_1 = \Theta_1^*$, while we let $0.4\Theta_2^* \leq \Theta_2 \leq \Theta_2^*$. We have plotted the achievable cost savings against the RE generation at site 2 in Fig. 12. As seen, daily savings of up to 1.37$ are achievable when the households are about 440m from the RE generation sites. Similarly, daily savings of up to 1.1$ are achievable when the households are about 550m from the generation sites.

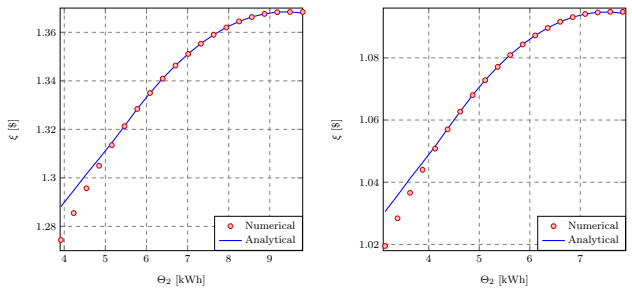

Fig. 12. Comparative performance: QP-REO vs. CoV-REO in a practical case. Cost savings plotted against RE generation at site 2. Left: Scenario 1 (households located 443.07 metres from each generation site). Right: Scenario 2 (households located 553,84 metres from each generation site).

The RE consumption schedules for the practical cases considered are shown in Fig. 13, where we have allowed $\Theta_1 = 0.7\Theta_1^*$ and $\Theta_2 = 0.7\Theta_2^*$. As observed, the RE consumption schedules are the same across households, this, given that the prices and power loss parameters are the same for all the participants. It is observed a fair similarity between the schedules obtained through QP-REO and CoV-REO. Moreover, the expected correlation of the RE consumption schedule with the prices offered is observed.

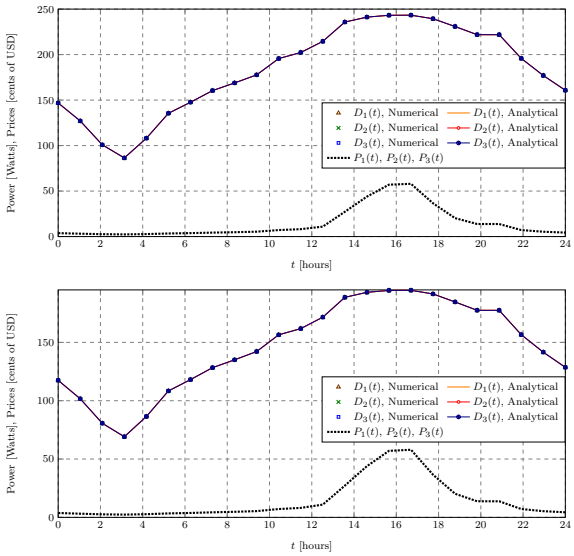

Fig. 13. Time-variation of RE consumption rate. Left: Scenario 1. Right: Scenario 2.

E. Additional Simulation Results

In this section we provide numerical results of various simulated scenarios in which 6 households share access to 2 RE generation sites. The simulation scenarios considered differ from each other in the power loss parameters of the connecting lines. Cases involving different distances between households and RE generation sites are considered. This, ultimately reflects on the choice of $K_{1,1}, \ldots, K_{6,1}$ and $K_{1,2}, \ldots, K_{6,2}$. The pricing signals in all the simulation scenarios are $P_1(\tau) = \sin(7\tau) + 2$, $P_2(\tau) = \cos(7\tau) + 2$, $P_3(\tau) = \sin(8\tau) + 2$, $P_4(\tau) = \sin(7\tau) + 2$, $P_5(\tau) = \cos(7\tau) + 2$, $P_6(\tau) = \sin(8\tau) + 2$. Moreover, in all scenarios, $M = 6$, $N = 2$, $S = 1$, $T = 30$, $\Delta t = 0.0345$, and the battery parameters are set as in Table III, except for the $J_n(0)$'s which are set according to the requirements stated in Sec. IV-B, i.e., $J_n(0) = \int_0^S R_n(\tau)d\tau$, $\forall\ n$. With these considerations, the simulation scenarios to consider are defined as follows:

- Scenario 1: $K_{1,1} = 0.05$, $K_{1,2} = 0.054545$, $K_{2,1} = 0.059091$, $K_{2,2} = 0.063636$, $K_{3,1} = 0.068182$, $K_{3,2} = 0.072727$, $K_{4,1} = 0.077273$, $K_{4,2} = 0.081818$, $K_{5,1} = 0.086364$, $K_{5,2} = 0.090909$, $K_{6,1} = 0.095455$, $K_{6,2} = 0.1$.
- Scenario 2: $K_{1,1} = 0.05$, $K_{1,2} = 0.063636$, $K_{2,1} = 0.077273$, $K_{2,2} = 0.090909$, $K_{3,1} = 0.104545$, $K_{3,2} = 0.118182$, $K_{4,1} = 0.131818$, $K_{4,2} = 0.145455$, $K_{5,1} = 0.159091$, $K_{5,2} = 0.172727$, $K_{6,1} = 0.186364$, $K_{6,2} = 0.2$.
- Scenario 3: $K_{1,1} = 0.01$, $K_{1,2} = 0.027273$, $K_{2,1} = 0.044545$, $K_{2,2} = 0.061818$, $K_{3,1} = 0.079091$, $K_{3,2} = 0.096364$, $K_{4,1} = 0.113636$, $K_{4,2} = 0.130909$, $K_{5,1} = 0.148182$, $K_{5,2} = 0.165455$, $K_{6,1} = 0.182727$, $K_{6,2} = 0.2$.

- Scenario 4: $K_{1,1} = 0.01$, $K_{1,2} = 0.018182$, $K_{2,1} = 0.026364$, $K_{2,2} = 0.034545$, $K_{3,1} = 0.042727$, $K_{3,2} = 0.050909$, $K_{4,1} = 0.059091$, $K_{4,2} = 0.067273$, $K_{5,1} = 0.075455$, $K_{5,2} = 0.083636$, $K_{6,1} = 0.091818$, $K_{6,2} = 0.1$.

The achievable savings obtained with the proposed strategies in the above mentioned scenarios are plotted against the RE production at the second generation site in Fig. 14. As observed, the scenario with the highest cost savings is Scenario 4, given that it features the smallest $K_{m,n}$ values. The scenario with the smallest cost savings is Scenario 2, as it has the largest values of $K_{m,n}$.

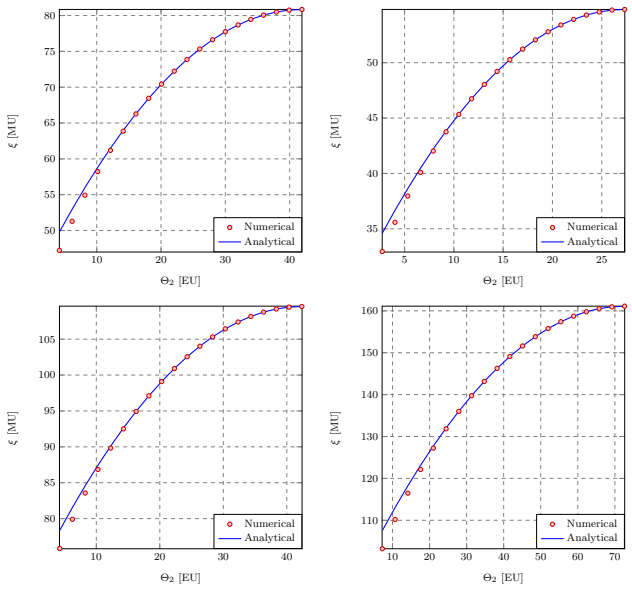

Fig. 14. Comparative performance: QP-REO vs. CoV-REO. Cost savings plotted against RE production at second generation site. Top-Left: Scenario 1. Top-Right: Scenario 2. Bottom-Left: Scenario 3. Bottom-Right: Scenario 4.

VII. Conclusions

We have proposed energy management strategies to minimize the cost incurred by a cooperating group of households over a finite planning horizon. The households share access to a group of RE generators and ESDs. In our framework we have taken into account the distance-dependent power loss incurred when transmitting energy from the RE generators to the loads. We have cast the optimization problem as a non-convex quadratically-constrained quadratic programming problem. We have then proposed solutions based on discretization, relaxation and variational methods. The approach based on variational methods has allowed us to obtain analytic results in closed form. We have presented a fair energy allocation policy to ensure full household cooperation over the entire planning horizon. Finally, we have discussed an ownership distribution which seeks to minimize the performance degradation incurred after imposing fairness-ensuring constraints.

The analytical results presented in this paper illustrate the relationship between the optimal RE consumption policy and system parameters such as the resistance of the lines connecting generators and loads, the distance between generators and loads, price variations across time and location, and RE generation capacity. These results can be used for energy planning purposes, while the proposed strategies can be used to benchmark and devise real-time energy management algorithms by incorporating forecasting techniques to estimate future RE generation and power consumption.

Appendix A
Cost Function as a Quadratic Form

The cost function χ can be approximated in terms of the vector $\mathbf{x}$ as $\chi \approx \Delta t\,[\epsilon - \mathbf{1}_M \mathbf{P}\mathbf{x} + \mathbf{x}^\intercal \mathbf{Q}\mathbf{K}\mathbf{x}]$, where:

$$\epsilon = \mathbf{1}_M \begin{bmatrix} \mathbf{p}_1^\intercal \boldsymbol{\ell}_1 \\ \vdots \\ \mathbf{p}_M^\intercal \boldsymbol{\ell}_M \end{bmatrix},$$

$$\mathbf{P} = \begin{pmatrix} (\mathbf{p}_1 \otimes \mathbf{1}_N) & 0 & \dots & 0 \\ 0 & (\mathbf{p}_2 \otimes \mathbf{1}_N) & \dots & 0 \\ \vdots & \vdots & \ddots & \vdots \\ 0 & 0 & \dots & (\mathbf{p}_M \otimes \mathbf{1}_N) \end{pmatrix},$$

$$\mathbf{Q} = \begin{pmatrix} \mathsf{dg}\,(\mathbf{p}_1 \otimes \mathbf{1}_N) & 0 & \dots & 0 \\ 0 & \mathsf{dg}\,(\mathbf{p}_2 \otimes \mathbf{1}_N) & \dots & 0 \\ \vdots & \vdots & \ddots & \vdots \\ 0 & 0 & \dots & \mathsf{dg}\,(\mathbf{p}_M \otimes \mathbf{1}_N) \end{pmatrix},$$

and

$$\mathbf{K} = \mathsf{dg}\,([\mathbf{k}_1, \mathbf{k}_2, \dots, \mathbf{k}_M])\,.$$

Appendix B
Constraints in Matrix Form

In this appendix we determine matrices $\mathbf{M}_1, \dots, \mathbf{M}_4$ and vectors $\mathbf{v}_1, \dots, \mathbf{v}_4$, which were introduced in Sec. IV-A to simplify the problem formulation.

From Eq. (4), it can be shown that $\mathbf{M}_1$ is given as follows:

$$\mathbf{M}_1 = \mathbf{1}_M \otimes \mathbf{I}_{NT},$$

where $\mathbf{1}_M$ is the vector of ones of length M, $\otimes$ denotes Kronecker product, and $\mathbf{I}_{NT}$ is the identity matrix of size $NT \times NT$.

Similarly, it follows from Eq. (4) that the vector $\mathbf{v}_1$ should be:

$$\mathbf{v}_1 = \begin{bmatrix} q_{D,1} \\ \vdots \\ q_{D,N} \\ \vdots\vdots \\ q_{D,1} \\ \vdots \\ q_{D,N} \end{bmatrix},$$

where the sequence $q_{D,1}, \dots, q_{D,N}$ repeats itself T times. To see how $\mathbf{M}_1\mathbf{x} \preceq \mathbf{v}_1$ is a discrete representation of Eq. (4), consider the example shown in Table IV, where $M = 4$, $N = 3$, $T = 2$. As seen, the first row implies:

$$D_{1,1}(\Delta t) + D_{2,1}(\Delta t) + D_{3,1}(\Delta t) + D_{4,1}(\Delta t) \leq q_{D,1},$$

TABLE IV
EXAMPLE OF $\mathbf{M}_1$ AND $\mathbf{v}_1$ WITH $M = 4$, $N = 3$, $T = 2$.

$$\begin{bmatrix} 1&0&0&0&0&0&1&0&0&0&0&0&0&1&0&0&0&0&0&0&1&0&0&0&0&0&0\\ 0&1&0&0&0&0&0&0&1&0&0&0&0&0&0&1&0&0&0&0&0&0&1&0&0&0&0\\ 0&0&1&0&0&0&0&0&0&1&0&0&0&0&0&0&1&0&0&0&0&0&0&1&0&0&0\\ 0&0&0&1&0&0&0&0&0&0&1&0&0&0&0&0&0&1&0&0&0&0&0&0&1&0&0\\ 0&0&0&0&1&0&0&0&0&0&0&1&0&0&0&0&0&0&1&0&0&0&0&0&0&1&0\\ 0&0&0&0&0&1&0&0&0&0&0&0&1&0&0&0&0&0&0&1&0&0&0&0&0&0&1 \end{bmatrix} \begin{bmatrix} D_{1,1}(\Delta t)\\ D_{1,2}(\Delta t)\\ D_{1,3}(\Delta t)\\ D_{1,1}(2\Delta t)\\ D_{1,2}(2\Delta t)\\ D_{1,3}(2\Delta t)\\ D_{2,1}(\Delta t)\\ D_{2,2}(\Delta t)\\ D_{2,3}(\Delta t)\\ D_{2,1}(2\Delta t)\\ D_{2,2}(2\Delta t)\\ D_{2,3}(2\Delta t)\\ D_{3,1}(\Delta t)\\ D_{3,2}(\Delta t)\\ D_{3,3}(\Delta t)\\ D_{3,1}(2\Delta t)\\ D_{3,2}(2\Delta t)\\ D_{3,3}(2\Delta t)\\ D_{4,1}(\Delta t)\\ D_{4,2}(\Delta t)\\ D_{4,3}(\Delta t)\\ D_{4,1}(2\Delta t)\\ D_{4,2}(2\Delta t)\\ D_{4,3}(2\Delta t) \end{bmatrix} \preceq \begin{bmatrix} q_{D,1}\\ q_{D,2}\\ q_{D,3}\\ q_{D,1}\\ q_{D,2}\\ q_{D,3} \end{bmatrix}$$

which is the same as Eq. (4) with $\tau = \Delta t$, and $M = 4$, $N = 3$.

As stated in Sec. IV-A, constraint (6) can be written in matrix form as $\mathbf{M}_2\mathbf{x} \preceq \mathbf{v}_2$, where $\mathbf{M}_2 = -\Delta t\,[\mathbf{1}_M \otimes (\mathbf{A}_T \otimes \boldsymbol{B}_N)]$, with:

$$\mathbf{A}_T = \begin{pmatrix} 1&0&0&\dots&0\\ 1&1&0&\dots&0\\ \vdots&\vdots&\vdots&\ddots&\vdots\\ 1&1&1&\dots&1 \end{pmatrix}_{T\times T},$$

$$\boldsymbol{B}_N = \begin{bmatrix} \frac{1}{\beta_1}&0&0&\dots&0\\ 0&\frac{1}{\beta_2}&0&\dots&0\\ 0&0&\frac{1}{\beta_3}&\dots&0\\ \vdots&\vdots&\vdots&\ddots&\vdots\\ 0&0&0&\dots&\frac{1}{\beta_N} \end{bmatrix}, \tag{32}$$

and

$$\mathbf{v}_2 = \begin{bmatrix} \Psi_1 - \alpha_1\Delta t\,(R_1(\Delta t)) - J_1(0)\\ \Psi_2 - \alpha_2\Delta t\,(R_2(\Delta t)) - J_2(0)\\ \vdots\\ \Psi_N - \alpha_N\Delta t\,(R_N(\Delta t)) - J_N(0)\\ \Psi_1 - \alpha_1\Delta t\,(R_1(\Delta t) + R_1(2\Delta t)) - J_1(0)\\ \Psi_2 - \alpha_2\Delta t\,(R_2(\Delta t) + R_2(2\Delta t)) - J_2(0)\\ \vdots\\ \Psi_N - \alpha_N\Delta t\,(R_N(\Delta t) + R_N(2\Delta t)) - J_N(0)\\ \vdots\\ \Psi_1 - \alpha_1\Delta t\left(\sum_{t=1}^{T} R_1(t\Delta t)\right) - J_1(0)\\ \Psi_2 - \alpha_2\Delta t\left(\sum_{t=1}^{T} R_2(t\Delta t)\right) - J_2(0)\\ \vdots\\ \Psi_N - \alpha_N\Delta t\left(\sum_{t=1}^{T} R_N(t\Delta t)\right) - J_N(0) \end{bmatrix}$$

To visualize why $\mathbf{M}_2\mathbf{x} \preceq \mathbf{v}_2$ is a valid discrete representation of constraint (6), readers are referred to the example shown in Table V, where we consider the case $M = 4$, $N = 3$, $T = 2$.

Given the similarities between constraints (6) and (7), it follows that $\mathbf{M}_3 = -\mathbf{M}_2$. The vector $\mathbf{v}_3$ is given as follows:

$$\mathbf{v}_3 = \begin{bmatrix} \alpha_1\Delta t\,(R_1(\Delta t)) + J_1(0)\\ \alpha_2\Delta t\,(R_2(\Delta t)) + J_2(0)\\ \vdots\\ \alpha_N\Delta t\,(R_N(\Delta t)) + J_N(0)\\ \alpha_1\Delta t\,(R_1(\Delta t) + R_1(2\Delta t)) + J_1(0)\\ \alpha_2\Delta t\,(R_2(\Delta t) + R_2(2\Delta t)) + J_2(0)\\ \vdots\\ \alpha_N\Delta t\,(R_N(\Delta t) + R_N(2\Delta t)) + J_N(0)\\ \vdots\\ \alpha_1\Delta t\left(\sum_{t=1}^{T} R_1(t\Delta t)\right) + J_1(0)\\ \alpha_2\Delta t\left(\sum_{t=1}^{T} R_2(t\Delta t)\right) + J_2(0)\\ \vdots\\ \alpha_N\Delta t\left(\sum_{t=1}^{T} R_N(t\Delta t)\right) + J_N(0) \end{bmatrix}$$

Again, to visualize why $\mathbf{M}_3\mathbf{x} \preceq \mathbf{v}_3$ is a valid discrete representation of constraint (7), readers are referred to the example shown in Table VI, where we consider the case $M = 4$, $N = 3$, $T = 2$.

As stated in Sec. IV-A, constraint (5) can be written in matrix form as $\mathbf{M}_4\mathbf{x} = \mathbf{v}_4$, where $\mathbf{M}_4 = -\Delta t\,[\mathbf{1}_M \otimes (\mathbf{1}_T \otimes \boldsymbol{B}_N)]$, with $\boldsymbol{B}_N$ as defined in (32), and

TABLE V
EXAMPLE OF $\mathbf{M}_2$ AND $\mathbf{v}_2$ WITH $M = 4$, $N = 3$, $T = 2$.

$$-\Delta t \begin{bmatrix} \frac{1}{\beta_1} & 0 & 0 & 0 & 0 & 0 & \frac{1}{\beta_1} & 0 & 0 & 0 & 0 & 0 & \frac{1}{\beta_1} & 0 & 0 & 0 & 0 & 0 & \frac{1}{\beta_1} & 0 & 0 & 0 & 0 & 0 \\ 0 & \frac{1}{\beta_2} & 0 & 0 & 0 & 0 & 0 & \frac{1}{\beta_2} & 0 & 0 & 0 & 0 & 0 & \frac{1}{\beta_2} & 0 & 0 & 0 & 0 & 0 & \frac{1}{\beta_2} & 0 & 0 & 0 & 0 \\ 0 & 0 & \frac{1}{\beta_3} & 0 & 0 & 0 & 0 & 0 & \frac{1}{\beta_3} & 0 & 0 & 0 & 0 & 0 & \frac{1}{\beta_3} & 0 & 0 & 0 & 0 & 0 & \frac{1}{\beta_3} & 0 & 0 & 0 \\ \frac{1}{\beta_1} & 0 & 0 & \frac{1}{\beta_1} & 0 & 0 & \frac{1}{\beta_1} & 0 & 0 & \frac{1}{\beta_1} & 0 & 0 & \frac{1}{\beta_1} & 0 & 0 & \frac{1}{\beta_1} & 0 & 0 & \frac{1}{\beta_1} & 0 & 0 & \frac{1}{\beta_1} & 0 & 0 \\ 0 & \frac{1}{\beta_2} & 0 & 0 & \frac{1}{\beta_2} & 0 & 0 & \frac{1}{\beta_2} & 0 & 0 & \frac{1}{\beta_2} & 0 & 0 & \frac{1}{\beta_2} & 0 & 0 & \frac{1}{\beta_2} & 0 & 0 & \frac{1}{\beta_2} & 0 & 0 & \frac{1}{\beta_2} & 0 \\ 0 & 0 & \frac{1}{\beta_3} & 0 & 0 & \frac{1}{\beta_3} & 0 & 0 & \frac{1}{\beta_3} & 0 & 0 & \frac{1}{\beta_3} & 0 & 0 & \frac{1}{\beta_3} & 0 & 0 & \frac{1}{\beta_3} & 0 & 0 & \frac{1}{\beta_3} & 0 & 0 & \frac{1}{\beta_3} \end{bmatrix} \begin{bmatrix} D_{1,1}(\Delta t) \\ D_{1,2}(\Delta t) \\ D_{1,3}(\Delta t) \\ D_{1,1}(2\Delta t) \\ D_{1,2}(2\Delta t) \\ D_{1,3}(2\Delta t) \\ D_{2,1}(\Delta t) \\ D_{2,2}(\Delta t) \\ D_{2,3}(\Delta t) \\ D_{2,1}(2\Delta t) \\ D_{2,2}(2\Delta t) \\ D_{2,3}(2\Delta t) \\ D_{3,1}(\Delta t) \\ D_{3,2}(\Delta t) \\ D_{3,3}(\Delta t) \\ D_{3,1}(2\Delta t) \\ D_{3,2}(2\Delta t) \\ D_{3,3}(2\Delta t) \\ D_{4,1}(\Delta t) \\ D_{4,2}(\Delta t) \\ D_{4,3}(\Delta t) \\ D_{4,1}(2\Delta t) \\ D_{4,2}(2\Delta t) \\ D_{4,3}(2\Delta t) \end{bmatrix} \geq$$

$$\begin{bmatrix} \Psi_1 - \alpha_1 \Delta t \left(R_1(\Delta t)\right) - J_1(0) \\ \Psi_2 - \alpha_2 \Delta t \left(R_2(\Delta t)\right) - J_2(0) \\ \Psi_3 - \alpha_3 \Delta t \left(R_3(\Delta t)\right) - J_3(0) \\ \Psi_1 - \alpha_1 \Delta t \left(R_1(\Delta t) + R_1(2\Delta t)\right) - J_1(0) \\ \Psi_2 - \alpha_2 \Delta t \left(R_2(\Delta t) + R_2(2\Delta t)\right) - J_2(0) \\ \Psi_3 - \alpha_3 \Delta t \left(R_3(\Delta t) + R_3(2\Delta t)\right) - J_3(0) \end{bmatrix}$$

TABLE VI
EXAMPLE OF $\mathbf{M}_3$ AND $\mathbf{v}_3$ WITH $M = 4$, $N = 3$, $T = 2$.

$$\Delta t \begin{bmatrix} \frac{1}{\beta_1} & 0 & 0 & 0 & 0 & 0 & \frac{1}{\beta_1} & 0 & 0 & 0 & 0 & 0 & \frac{1}{\beta_1} & 0 & 0 & 0 & 0 & 0 & \frac{1}{\beta_1} & 0 & 0 & 0 & 0 & 0 \\ 0 & \frac{1}{\beta_2} & 0 & 0 & 0 & 0 & 0 & \frac{1}{\beta_2} & 0 & 0 & 0 & 0 & 0 & \frac{1}{\beta_2} & 0 & 0 & 0 & 0 & 0 & \frac{1}{\beta_2} & 0 & 0 & 0 & 0 \\ 0 & 0 & \frac{1}{\beta_3} & 0 & 0 & 0 & 0 & 0 & \frac{1}{\beta_3} & 0 & 0 & 0 & 0 & 0 & \frac{1}{\beta_3} & 0 & 0 & 0 & 0 & 0 & \frac{1}{\beta_3} & 0 & 0 & 0 \\ \frac{1}{\beta_1} & 0 & 0 & \frac{1}{\beta_1} & 0 & 0 & \frac{1}{\beta_1} & 0 & 0 & \frac{1}{\beta_1} & 0 & 0 & \frac{1}{\beta_1} & 0 & 0 & \frac{1}{\beta_1} & 0 & 0 & \frac{1}{\beta_1} & 0 & 0 & \frac{1}{\beta_1} & 0 & 0 \\ 0 & \frac{1}{\beta_2} & 0 & 0 & \frac{1}{\beta_2} & 0 & 0 & \frac{1}{\beta_2} & 0 & 0 & \frac{1}{\beta_2} & 0 & 0 & \frac{1}{\beta_2} & 0 & 0 & \frac{1}{\beta_2} & 0 & 0 & \frac{1}{\beta_2} & 0 & 0 & \frac{1}{\beta_2} & 0 \\ 0 & 0 & \frac{1}{\beta_3} & 0 & 0 & \frac{1}{\beta_3} & 0 & 0 & \frac{1}{\beta_3} & 0 & 0 & \frac{1}{\beta_3} & 0 & 0 & \frac{1}{\beta_3} & 0 & 0 & \frac{1}{\beta_3} & 0 & 0 & \frac{1}{\beta_3} & 0 & 0 & \frac{1}{\beta_3} \end{bmatrix} \begin{bmatrix} D_{1,1}(\Delta t) \\ D_{1,2}(\Delta t) \\ D_{1,3}(\Delta t) \\ D_{1,1}(2\Delta t) \\ D_{1,2}(2\Delta t) \\ D_{1,3}(2\Delta t) \\ D_{2,1}(\Delta t) \\ D_{2,2}(\Delta t) \\ D_{2,3}(\Delta t) \\ D_{2,1}(2\Delta t) \\ D_{2,2}(2\Delta t) \\ D_{2,3}(2\Delta t) \\ D_{3,1}(\Delta t) \\ D_{3,2}(\Delta t) \\ D_{3,3}(\Delta t) \\ D_{3,1}(2\Delta t) \\ D_{3,2}(2\Delta t) \\ D_{3,3}(2\Delta t) \\ D_{4,1}(\Delta t) \\ D_{4,2}(\Delta t) \\ D_{4,3}(\Delta t) \\ D_{4,1}(2\Delta t) \\ D_{4,2}(2\Delta t) \\ D_{4,3}(2\Delta t) \end{bmatrix} \geq$$

$$\begin{bmatrix} \alpha_1 \Delta t \left(R_1(\Delta t)\right) + J_1(0) \\ \alpha_2 \Delta t \left(R_2(\Delta t)\right) + J_2(0) \\ \alpha_3 \Delta t \left(R_3(\Delta t)\right) + J_3(0) \\ \alpha_1 \Delta t \left(R_1(\Delta t) + R_1(2\Delta t)\right) + J_1(0) \\ \alpha_2 \Delta t \left(R_2(\Delta t) + R_2(2\Delta t)\right) + J_2(0) \\ \alpha_3 \Delta t \left(R_3(\Delta t) + R_3(2\Delta t)\right) + J_3(0) \end{bmatrix}$$

$\mathbf{v}_4$ given as follows:

$$\mathbf{v}_4 = \begin{bmatrix} \alpha_1 \Delta t \left(\sum_{t=1}^{T} R_1(t\Delta t) \right) \\ \alpha_2 \Delta t \left(\sum_{t=1}^{T} R_2(t\Delta t) \right) \\ \vdots \\ \alpha_N \Delta t \left(\sum_{t=1}^{T} R_N(t\Delta t) \right) \end{bmatrix}$$

To visualize why $\mathbf{M}_4\mathbf{x} = \mathbf{v}_4$ is a valid discrete representation of constraint (5), readers are referred to the example shown in Table VII, where we consider the case $M = 4$, $N = 3$, $T = 2$.

APPENDIX C
PROOF OF THEOREM 1

Proof. First, we will show that ξ is concave in λ_n by computing the second order derivative $\frac{\partial^2}{\partial \lambda_n^2}\xi$, which is always negative whenever $K_{m,n} > 0$ and $P_m(\tau) > 0,\ \forall\ m,\ \forall\ n,\ \forall\ \tau$. The first derivative of ξ with respect to λ_n can be computed from Eq. (18) in the paper:

$$\frac{\partial}{\partial \lambda_n}\xi = \frac{\partial}{\partial \lambda_n} \sum_{m=1}^{M} \int_0^S \sum_{n=1}^{N} P_m(\tau) \left[D_{m,n}(\tau) - K_{m,n} D_{m,n}^2(\tau) \right] d\tau,$$

which yields:

$$\frac{\partial}{\partial \lambda_n}\xi = 2 \sum_{m=1}^{M} \frac{S}{4K_{m,n}} - \lambda_n \frac{1}{4K_{m,n}} \int_0^S \frac{1}{P_m(\tau)} d\tau - \frac{S}{4K_{m,n}}.$$

The quantity $\frac{\partial^2}{\partial \lambda_n^2}\xi$ can be obtained by differentiating the expression above with respect to λ_n:

$$\frac{\partial^2}{\partial \lambda_n^2}\xi = -\sum_{m=1}^{M} \frac{1}{2K_{m,n}} \int_0^S \frac{1}{P_m(\tau)} d\tau.$$

Now note that λ_n is a linear and decreasing function of Θ_n, which can be written as $\lambda_n = a - b\Theta_n$ for some $a \in \mathbb{R}$ and $b \in \mathbb{R}$. The composition with affine functions preserves concavity [49], as a result, the function $\xi\left[\lambda_1(\Theta_1), \ldots, \lambda_N(\Theta_N)\right]$ is concave in Θ_n. ■

REFERENCES

[1] J. Pan *et al.*, "An Internet of Things framework for smart energy in buildings: Designs, prototype, and experiments," *IEEE Internet of Things Journal*, vol. 2, no. 6, pp. 527–537, Dec 2015.

[2] A. Zanella *et al.*, "Internet of Things for smart cities," *IEEE Internet of Things Journal*, vol. 1, no. 1, pp. 22–32, Feb 2014.

[3] Y. Wang *et al.*, "Distributed online algorithm for optimal real-time energy distribution in the smart grid," *IEEE Internet of Things Journal*, vol. 1, no. 1, pp. 70–80, Feb 2014.

[4] G. Xu *et al.*, "Toward integrating distributed energy resources and storage devices in smart grid," *IEEE Internet of Things Journal*, vol. 4, no. 1, pp. 192–204, Feb 2017.

[5] M. Moness and A. M. Moustafa, "A survey of cyber-physical advances and challenges of wind energy conversion systems: Prospects for Internet of energy," *IEEE Internet of Things Journal*, vol. 3, no. 2, pp. 134–145, April 2016.

[6] D. Feldman *et al.*, "Shared Solar: Current Landscape, Market Potential, and the Impact of Federal Securities Regulation," Tech. Rep. NREL/TP-6A20-63892, 2015. [Online]. Available: https://www.nrel.gov/docs/fy15osti/63892.pdf

[7] P. Augustine and E. McGavisk, "The next big thing in renewable energy: Shared solar," *The Electricity Journal*, vol. 29, no. 4, pp. 36 – 42, 2016. [Online]. Available: http://www.sciencedirect.com/science/article/pii/S104061901630029X

[8] D. An *et al.*, "Sto2auc: A stochastic optimal bidding strategy for microgrids," *IEEE Internet of Things Journal*, vol. 4, no. 6, pp. 2260–2274, Dec 2017.

[9] G. Ye *et al.*, "Towards cost minimization with renewable energy sharing in cooperative residential communities," *IEEE Access*, vol. 5, pp. 11 688–11 699, 2017.

[10] C. Yang *et al.*, "On demand response management performance optimization for microgrids under imperfect communication constraints," *IEEE Internet of Things Journal*, vol. 4, no. 4, pp. 881–893, Aug 2017.

[11] L. Yu *et al.*, "Carbon-aware energy cost minimization for distributed Internet data centers in smart microgrids," *IEEE Internet of Things Journal*, vol. 1, no. 3, pp. 255–264, June 2014.

[12] A. C. Luna *et al.*, "Cooperative energy management for a cluster of households prosumers," *IEEE Trans. Consumer Electronics*, vol. 62, no. 3, pp. 235–242, August 2016.

[13] K. Rahbar *et al.*, "Energy cooperation optimization in microgrids with renewable energy integration," *IEEE Trans. Smart Grid*, vol. PP, no. 99, pp. 1–1, 2016.

[14] H. Dagdougui *et al.*, "Global energy management system for cooperative networked residential green buildings," *IET Renewable Power Generation*, vol. 10, no. 8, pp. 1237–1244, 2016.

[15] Z. Wang *et al.*, "Active demand response using shared energy storage for household energy management," *IEEE Trans. on Smart Grid*, vol. 4, no. 4, pp. 1888–1897, Dec 2013.

[16] I. Atzeni *et al.*, "Demand-side management via distributed energy generation and storage optimization," *IEEE Trans. on Smart Grid*, vol. 4, no. 2, pp. 866–876, June 2013.

[17] W. Tushar *et al.*, "Management of renewable energy for a shared facility controller in smart grid," *IEEE Access*, vol. 4, pp. 4269–4281, 2016.

[18] A. Parisio *et al.*, "Cooperative MPC-based energy management for networked microgrids," *IEEE Trans. on Smart Grid*, vol. 8, no. 6, pp. 3066–3074, Nov 2017.

[19] C. P. Mediwaththe *et al.*, "A dynamic game for electricity load management in neighborhood area networks," *IEEE Trans. on Smart Grid*, vol. 7, no. 3, pp. 1329–1336, May 2016.

[20] A. Chiş and V. Koivunen, "Coalitional game based cost optimization of energy portfolio in smart grid communities," *IEEE Trans. on Smart Grid*, vol. PP, no. 99, pp. 1–1, 2017.

[21] J. Leithon *et al.*, "Demand response and renewable energy management using continuous-time optimization," *IEEE Trans. on Sustainable Energy*, vol. PP, no. 99, pp. 1–1, 2017.

[22] Z. Huang *et al.*, "Minimizing transmission loss in smart microgrids by sharing renewable energy," *ACM Trans. Cyber-Phys. Syst.*, vol. 1, no. 2, pp. 5:1–5:22, Dec. 2016. [Online]. Available: http://doi.acm.org/10.1145/2823355

[23] Z. Zhou *et al.*, "Game-theoretical energy management for energy Internet with big data-based renewable power forecasting," *IEEE Access*, vol. 5, pp. 5731–5746, 2017.

[24] H. K. Nunna *et al.*, "Multi-agent based demand response management system for combined operation of smart microgrids," *Sustainable Energy, Grids and Networks*, vol. 6, no. Supplement C, pp. 25 – 34, 2016. [Online]. Available: http://www.sciencedirect.com/science/article/pii/S2352467716000035

[25] J. Rajasekharan and V. Koivunen, "Optimal energy consumption model for smart grid households with energy storage," *IEEE Journal of Sel. Topics in Signal Processing*, vol. 8, no. 6, pp. 1154–1166, Dec 2014.

[26] Y. Zhang *et al.*, "Day-ahead smart grid cooperative distributed energy scheduling with renewable and storage integration," *IEEE Trans. on Sustainable Energy*, vol. 7, no. 4, pp. 1739–1748, Oct 2016.

[27] G. Binetti *et al.*, "Distributed consensus-based economic dispatch with transmission losses," *IEEE Trans. on Power Systems*, vol. 29, no. 4, pp. 1711–1720, July 2014.

[28] C. Zhao *et al.*, "Consensus-based energy management in smart grid with transmission losses and directed communication," *IEEE Trans. on Smart Grid*, vol. 8, no. 5, pp. 2049–2061, Sept 2017.

[29] T. C. Chiu *et al.*, "Optimized day-ahead pricing with renewable energy demand-side management for smart grids," *IEEE Internet of Things Journal*, vol. 4, no. 2, pp. 374–383, April 2017.

[30] M. Rastegar *et al.*, "A probabilistic energy management scheme for renewable-based residential energy hubs," *IEEE Trans. Smart Grid*, vol. PP, no. 99, pp. 1–11, 2016.

TABLE VII
EXAMPLE OF $\mathbf{M}_4$ AND $\mathbf{v}_4$ WITH $M = 4$, $N = 3$, $T = 2$.

$$\Delta t \begin{bmatrix} \frac{1}{\beta_1} & 0 & 0 & \frac{1}{\beta_1} & 0 & 0 & \frac{1}{\beta_1} & 0 & 0 & \frac{1}{\beta_1} & 0 & 0 & \frac{1}{\beta_1} & 0 & 0 & \frac{1}{\beta_1} & 0 & 0 & \frac{1}{\beta_1} & 0 & 0 & \frac{1}{\beta_1} & 0 & 0 \\ 0 & \frac{1}{\beta_2} & 0 & 0 & \frac{1}{\beta_2} & 0 & 0 & \frac{1}{\beta_2} & 0 & 0 & \frac{1}{\beta_2} & 0 & 0 & \frac{1}{\beta_2} & 0 & 0 & \frac{1}{\beta_2} & 0 & 0 & \frac{1}{\beta_2} & 0 & 0 & \frac{1}{\beta_2} & 0 \\ 0 & 0 & \frac{1}{\beta_3} & 0 & 0 & \frac{1}{\beta_3} & 0 & 0 & \frac{1}{\beta_3} & 0 & 0 & \frac{1}{\beta_3} & 0 & 0 & \frac{1}{\beta_3} & 0 & 0 & \frac{1}{\beta_3} & 0 & 0 & \frac{1}{\beta_3} & 0 & 0 & \frac{1}{\beta_3} \end{bmatrix} \begin{bmatrix} D_{1,1}(\Delta t) \\ D_{1,2}(\Delta t) \\ D_{1,3}(\Delta t) \\ D_{1,1}(2\Delta t) \\ D_{1,2}(2\Delta t) \\ D_{1,3}(2\Delta t) \\ D_{2,1}(\Delta t) \\ D_{2,2}(\Delta t) \\ D_{2,3}(\Delta t) \\ D_{2,1}(2\Delta t) \\ D_{2,2}(2\Delta t) \\ D_{2,3}(2\Delta t) \\ D_{3,1}(\Delta t) \\ D_{3,2}(\Delta t) \\ D_{3,3}(\Delta t) \\ D_{3,1}(2\Delta t) \\ D_{3,2}(2\Delta t) \\ D_{3,3}(2\Delta t) \\ D_{4,1}(\Delta t) \\ D_{4,2}(\Delta t) \\ D_{4,3}(\Delta t) \\ D_{4,1}(2\Delta t) \\ D_{4,2}(2\Delta t) \\ D_{4,3}(2\Delta t) \end{bmatrix} =$$

$$\begin{bmatrix} \alpha_1 \Delta t \left(R_1(\Delta t) + R_1(2\Delta t) \right) \\ \alpha_2 \Delta t \left(R_2(\Delta t) + R_2(2\Delta t) \right) \\ \alpha_3 \Delta t \left(R_3(\Delta t) + R_3(2\Delta t) \right) \end{bmatrix}$$

[31] T. Li and M. Dong, "Real-time energy storage management with renewable integration: Finite-time horizon approach," *IEEE J. Sel. Areas in Commun.*, vol. 33, no. 12, pp. 2524–2539, Dec 2015.

[32] D. Liu *et al.*, "Residential energy scheduling for variable weather solar energy based on adaptive dynamic programming," *IEEE/CAA Journal of Automatica Sinica*, vol. 5, no. 1, pp. 36–46, Jan 2018.

[33] V. Pilloni *et al.*, "Smart home energy management including renewable sources: A QoE-driven approach," *IEEE Trans. Smart Grid*, vol. PP, no. 99, pp. 1–1, 2017.

[34] S. Grillo *et al.*, "Optimal management strategy of a battery-based storage system to improve renewable energy integration in distribution networks," *IEEE Trans. Smart Grid*, vol. 3, no. 2, pp. 950–958, June 2012.

[35] P. Peterson Drake and F. J. Fabozzi, *The basics of finance: an introduction to financial markets, business finance, and portfolio management*. Hoboken, NJ: Wiley, 2010.

[36] J. Leithon *et al.*, "Online demand response strategies for non-deferrable loads with renewable energy," *IEEE Trans. Smart Grid*, vol. PP, 2017.

[37] ——, "Renewable energy optimization with centralized and distributed generation," in *2018 26th European Signal Processing Conference (EUSIPCO)*, Sept. 2018.

[38] Z. Shu and P. Jirutitijaroen, "Optimal operation strategy of energy storage system for grid-connected wind power plants," *IEEE Trans. on Sustainable Energy*, vol. 5, no. 1, pp. 190–199, Jan 2014.

[39] H. Bao and R. Lu, "A new differentially private data aggregation with fault tolerance for smart grid communications," *IEEE Internet of Things Journal*, vol. 2, no. 3, pp. 248–258, June 2015.

[40] D. Minoli *et al.*, "Iot considerations, requirements, and architectures for smart buildings—energy optimization and next-generation building management systems," *IEEE Internet of Things Journal*, vol. 4, no. 1, pp. 269–283, Feb 2017.

[41] Q. Sun *et al.*, "A comprehensive review of smart energy meters in intelligent energy networks," *IEEE Internet of Things Journal*, vol. 3, no. 4, pp. 464–479, Aug 2016.

[42] J. Gondzio, "Interior point methods 25 years later," *European Journal of Operational Research*, vol. 218, no. 3, p. 587, 2011;2012;.

[43] M. Giaquinta *et al.*, *Calculus of Variations I*. Berlin, Heidelberg: Springer Berlin Heidelberg, 2004, vol. 310.

[44] Y. Nesterov and S. O. service), *Lectures on Convex Optimization*, 2nd ed. Cham: Springer International Publishing, 2018, vol. 137;137.;.

[45] SunPower, "E-Series Residential Solar Panels, E20-327," 2016, Accessed Dec. 2018. [Online]. Available: https://global.sunpower.com/sites/international/files/media-library/data-sheets/ds-spr-e20-327-320-residential-datasheet.pdf

[46] Power-Sonic Corporation, "Sealed Lead Acid Batteries Technical Manual," 2009, Accessed Dec. 2018. [Online]. Available: {http://www.power-sonic.com/images/powersonic/technical/1277751263_20100627-TechManual-Lo.pdf}

[47] Victron Energy, "AWG to Metric Conversion Chart," Accessed Dec. 2018. [Online]. Available: https://www.victronenergy.com/TechnicalInfo/TechPDF/AWG%20toMetric%20Conversion%20Chart.pdf

[48] Southern California Edison, "TOU-GS-2-RTP General service-medium real time pricing," 2017, Accessed Dec. 2018. [Online]. Available: https://www.sce.com/NR/sc3/tm2/pdf/CE331.pdf

[49] S. Boyd and L. Vandenberghe, *Convex Optimization*. New York, NY, USA: Cambridge University Press, 2004.